Chiral phases of superfluid ^{3}He in an anisotropic medium

J. A. Sauls

Department of Physics and Astronomy, Northwestern University, Evanston, Illinois 60208, USA

(Received 19 September 2012; revised manuscript received 8 September 2013; published 2 December 2013)

Recent advances in the fabrication and characterization of *anisotropic* silica aerogels with exceptional homogeneity provide new insight into the nature of unconventional pairing in disordered anisotropic media. I report theoretical analysis and predictions for the equilibrium phases of superfluid ^{3}He infused into a low-density, homogeneous uniaxial aerogel. Ginzburg-Landau (GL) theory for a class of equal-spin-pairing (ESP) states in a medium with uniaxial anisotropy is developed and used to analyze recent experiments on uniaxially strained aerogels. For ^{3}He in an axially "stretched" aerogel, GL theory predicts a transition from normal liquid into a *chiral* Anderson-Morel phase at T_{c_1} in which the chirality axis $\hat{\mathbf{l}}$ is aligned *along* the strain axis. This orbitally aligned state is protected from random fluctuations in the anisotropy direction, has a positive nuclear magnetic resonance (NMR) frequency shift, a sharp NMR resonance line, and is identified with the high-temperature ESP-1 phase of superfluid ^{3}He in axially stretched aerogel. A second transition into a biaxial phase is predicted to onset at a slightly lower temperature $T_{c_2} < T_{c_1}$. This phase is an ESP state, breaks time-reversal symmetry, and is defined by an orbital order parameter that spontaneously breaks axial rotation symmetry. This transition is driven by the coupling of an axially aligned one-dimensional "polar" order parameter to the two time-reversed two-dimensional axial Anderson-Brinkman-Morel states. The biaxial phase has a continuous degeneracy associated with the projection of its chiral axis in the plane normal to the anisotropy axis. Theoretical predictions for the NMR frequency shifts of the biaxial phase provide an identification of the ESP-2 as the biaxial state, partially *disordered* by random anisotropy (Larkin-Imry-Ma effect). The "width" of the jump in the NMR frequency shift at T_{c_2} provides an estimate of the orbital domain size $\xi_{\rm LIM} \simeq 5\ \mu$m at 18 bar. I show that the random anisotropy results from mesoscopic structures in silica aerogels. This model for the random anisotropy field is coarse grained on the atomic scale, and is formulated in terms of local anisotropy in the scattering of quasiparticles in an aerogel with orientational correlations. Long-range order of locally anisotropic scattering centers is related to the splitting of the two ESP phases.

DOI: 10.1103/PhysRevB.88.214503 PACS number(s): 67.30.ef, 67.30.hm, 67.30.hj

The discovery of superfluidity of ^{3}He infused into high-porosity silica *aerogel* opened a new chapter into the complex ordered phases of liquid ^{3}He and provided a novel method to study the effects of quenched disorder on the symmetry and stability of unconventional pairing states in Fermi superfluids.[1,2] The nature of the ordered phases of ^{3}He in high-porosity aerogel has recently been clarified by experiments using silica aerogels with high homogeneity.[3]

Nuclear magnetic resonance (NMR) spectroscopy has proven to be a powerful diagnostic of the symmetry of the order parameter for the superfluid phases.[4] Pulsed NMR experiments on ^{3}He infused into a *uniformly isotropic aerogel* with 98.2% porosity[5] provide an unambiguous identification of the order parameter as a Balian-Werthamer (BW) state,[6] albeit with a significantly reduced order-parameter amplitude $\Delta_{\rm B}(T)$ and longitudinal resonance frequency $\Omega_{\rm B}(T)$, compared to that in bulk ^{3}He-B. Unlike the B phase of pure ^{3}He, which has a fully gapped excitation spectrum, analyses of heat capacity,[7] thermal conductivity,[8] and magnetization measurements[9] show that the B phase of ^{3}He-aerogel is *gapless*, with disorder-induced Andreev states dominating the low-temperature thermal and transport properties.[10] The suppression of the A phase and the absence of a polycritical point (PCP) in isotropic aerogels is consistent with theoretical predictions based on pair breaking by scattering from a homogeneous distribution of isotropic impurities or a distribution of weakly anisotropic impurities with orientational correlations on length scale $\xi_{\rm s}$ less than the pair correlation length $\xi_0 = \hbar v_f/2\pi k_{\rm B} T_c$.[11–13]

The fabrication of *anisotropic* aerogels with exceptional homogeneity[3] has led to recent superflow and NMR experiments that provide a clearer understanding of the nature of the superfluid phases of ^{3}He in homogeneous silica aerogels. Anisotropic stress acting on a homogeneously isotropic aerogel can dramatically alter the relative stability of anisotropic pairing states by favoring one or more orbital components of the p-wave order parameter.[11–14] Indeed, the sensitivity of the order parameter to uniaxial strain is exhibited in torsional oscillator experiments performed on ^{3}He confined in axially compressed aerogel.[15] These experiments show a large metastable region of the phase diagram upon cooling, *assumed* to be the chiral Anderson-Brinkman-Morel (ABM) state[16,17] (A phase), that extends well below the bulk PCP. Upon warming from the low-temperature phase, presumed to be an anisotropic B phase, the transition into the high-temperature A phase occurs at $T_{\rm AB} = 0.075$ mK below the onset of superfluidity in the aerogel ($T_{c_a} = 2.275$ mK at $p = 31.9$ bar). This transition is absent for ^{3}He in uncompressed isotropic aerogel, and is interpreted as the transition into an *equilibrium* ABM state stabilized by uniaxial strain.[15] However, identification of the high-temperature superfluid phase as the ABM state is not established. Measurements of the superfluid density are insufficient to determine the symmetry of the order parameter. Additional NMR experiments should clarify the symmetry of the ordered phases of ^{3}He in uniformly anisotropic, compressed aerogels.

NMR experiments on ^{3}He infused into uniformly anisotropic, "axially stretched" aerogel[18] lead to a radically different phase diagram and interpretation of the ordered phases than what is found for ^{3}He in isotropic aerogels.[19] Two distinct superfluid phases, both equal-spin-pairing (ESP)

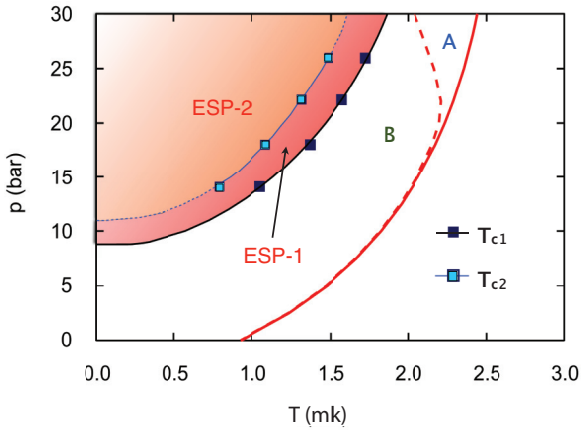

FIG. 1. (Color online) Two equal-spin-pairing phases labeled ESP-1 (pink region) and ESP-2 (orange region) identify the ordered phases of ^{3}He in uniaxially stretched aerogel with 97.5% porosity (adapted from Ref. 19). The transition at T_{c_1} is substantially reduced below the bulk transition (red line). The second ESP state onsets at T_{c_2}. An A-B transition at high pressure, characteristic of bulk ^{3}He (dotted red line), is not observed.

states, are observed. The phase for $T_{c_2} < T < T_{c_1}$ (ESP-1 in Fig. 1) was identified as an ABM state with the chiral axis aligned *perpendicular* to both the strain axis ($\hat{\mathbf{z}}$) and the magnetic field, i.e., the "easy-plane" configuration with $\hat{\mathbf{l}} \perp \hat{\mathbf{z}}$. This identification is based on the observations of (i) a positive NMR frequency shift with linewidth as narrow as the normal-state Larmor resonance, (ii) a tipping angle dependence of the NMR shift in agreement with that predicted for the ABM state, and (iii) a theoretical model based on *strain alignment of random cylinders* to describe the local anisotropic structure of aerogel.[20] This model is combined with the theory of Rainer and Vuorio[21] for the orientation energy of the chiral axis of *pure* ^{3}He-A by a *single* cylindrical impurity, which then predicts the chiral axis to align *with* the strain axis for compressed aerogels, i.e., "easy axis" with $\hat{\mathbf{l}} \parallel \hat{\mathbf{z}}$ for $\epsilon_{zz} < 0$, and *perpendicular* to the strain axis for stretched aerogel, i.e., "easy plane" with $\hat{\mathbf{l}} \perp \hat{\mathbf{z}}$ for $\epsilon_{zz} > 0$.[20,22,23] This alignment model underlies the interpretation of the ordered phases for ^{3}He in uniaxially strained aerogels reported by several groups.[15,19,24] However, the identification of uniaxial compression (stretching) with "easy-axis" ("easy-plane") alignment of the chiral axis is model dependent, in this case, upon the alignment of rigid cylinders representing the local anisotropy of otherwise globally isotropic aerogel and the assumption that the single impurity result of Ref. 21 extends to a distribution cylindrical impurities with typical spacing ξ_a that is less than or the same order as the pair correlation length ξ_0. Indeed, the fractal structure of the aerogel[25–27] on length scales shorter than ξ_a implies that the orientation of the chiral axis may not be inferred from the orientation energy characteristic of a single cylindrical impurity in pure ^{3}He. Furthermore, the response of a fractal network of silica strands and clusters to an external force applied at the surface of an aerogel is a complex problem. The local stress distribution, changes in bond angles, etc., may be very different from that based on rotation alignment of rigid cylindrical impurities.[28,29]

In Sec. I, I step back from a microscopic description of how global anisotropy is connected with local anisotropy and atomic forces, and consider the symmetry constraints for the phases of superfluid ^{3}He embedded in a uniformly anisotropic medium on the scale of the pair correlation length $\xi(T)$ and develop a Ginzburg-Landau (GL) theory for ESP phases in such a medium. These considerations lead to predictions for the order parameter and their NMR signatures for the phases of superfluid ^{3}He infused into uniaxially stretched aerogel. In Secs. II and III, I provide theoretical analysis for the identification of the ESP-1 phase as an ABM state with the chiral axis aligned *along* the strain axis. A second transition into a biaxial phase is predicted to onset at a slightly lower temperature $T_{c_2} < T_{c_1}$ (Sec. V). This ESP phase breaks time-reversal symmetry, and is defined by a chiral orbital order parameter that spontaneously breaks axial rotation symmetry. This transition is driven by the coupling of an axially aligned one-dimensional (1D) "polar" order parameter to the two time-reversed two-dimensional (2D) axial ABM states. The biaxial phase has a continuous degeneracy associated with the projection of its chiral axis in the plane normal to the anisotropy axis. In Sec. VI, I show that the NMR signatures of the ESP-2 phase are explained by a partially disordered biaxial phase in which the chiral axis is disordered on a *cone*, centered on the strain axis, by the random anisotropy of the aerogel medium, the Larkin-Imry-Ma (LIM) effect.[20,30,31] I also include a discussion of the possibility of a normal to 1D polar transition for ^{3}He in a strongly anisotropic aerogel in Sec. IV, as well as why this scenario does not explain the phase diagram of Ref. 19. In Secs. VII and VIII, the GL theory is combined with microscopic theory for pair breaking in a medium with both random and global anisotropy. This allows for additional predictions connecting the normal-state transport properties of ^{3}He in anisotropic aerogels with the symmetry of the superfluid phases. In particular, in Sec. IX, I discuss a model for random anisotropy and the LIM effect within a scattering theory of partially ordered anisotropic impurities. This model is the basis for the partially disordered biaxial phase that is identified with the ESP-2 phase.

I. GL THEORY FOR ^{3}He IN UNIAXIAL AEROGEL

The normal phase of pure liquid ^{3}He is separately invariant under spin and orbital rotations, gauge transformations $[U(1)_N]$, as well as discrete symmetries of space (P) and time (T) inversion, i.e., the group is $G = SO(3)_S \times SO(3)_L \times U(1)_N \times P \times T$.[32] The order parameter for pure ^{3}He belongs to vector representations of both spin and orbital rotation groups $SO(3)_S$ and $SO(3)_L$. The 2×2 matrix representation for the spin-triplet, p-wave order parameter[6,33]

$$\Delta_{\alpha\beta}(\hat{\mathbf{p}}) = \vec{\mathbf{d}}(\hat{\mathbf{p}}) \cdot (i\vec{\boldsymbol{\sigma}}\sigma_y)_{\alpha\beta} \tag{1}$$

is parametrized by $\vec{\mathbf{d}}(\hat{\mathbf{p}})$, which transforms as a vector under $SO(3)_S$, while the orbital pairing states are a superposition of the $L = 1$ basis $\{\hat{p}_i \,|\, i = x,y,z\}$ of $SO(3)_L$, i.e., $\mathbf{d}_\alpha(\hat{\mathbf{p}}) = \sum_i A_{\alpha i}\,(\hat{\mathbf{p}}_i)$.[34]

The superfluid phases of ^{3}He in "stretched" aerogel are identified as ESP states.[19] Here, I consider the class of ESP states of the form $A_{\alpha i} = \mathbf{d}_\alpha \mathscr{A}_i$, where $\vec{\mathbf{d}}$ is a real unit vector in spin space orthogonal to the plane of the Cooper-pair spins, and $\mathscr{A}_i$ is a complex vector under orbital rotations.

For ^{3}He embedded in a homogeneous, nonmagnetic, anisotropic medium with inversion symmetry, the orbital rotation symmetry is reduced, and the 3D basis $\{\mathscr{A}_i \mid i = x,y,z\}$ for the vector representation of $SO(3)_L$ is reduced to bases for 2D and 1D irreducible representations of $SO(2)_{L_z} \times Z_2$:

$$\begin{pmatrix} \mathscr{A}_x \\ \mathscr{A}_y \\ \mathscr{A}_z \end{pmatrix} \xrightarrow[\text{strain}]{\text{uniaxial}} \underset{(b)}{\begin{pmatrix} a_x \\ a_y \end{pmatrix}}, \tag{2}$$

where Z_2 represents the identity and a π rotation about an axis perpendicular to the uniaxial strain axis (R_π), the latter denoted as $\hat{\mathbf{z}}$. The 1D order parameter is the "polar" state, which is invariant under $SO(2)_{L_z}$ and changes sign for $b \xrightarrow{R_\pi} -b$. The maximal symmetry group is then $G' = SO(3)_S \times SO(2)_{L_z} \times Z_2 \times U(1)_N \times P \times T$. For each irreducible representation, there is a second-order invariant for the leading-order contribution to the Ginzburg-Landau functional. For the class of ESP states, there is one fourth-order invariant for the 1D representation, two fourth-order invariants for the 2D orbital representation, and two mixed-symmetry invariants. Thus, the GL functional for zero magnetic field is

$$\begin{aligned} \Delta\Omega[\vec{a},b] = {} & \alpha_\perp(T)\,|\vec{a}|^2 + \alpha_\parallel(T)\,|b|^2 \\ & + \beta_1\,|\vec{a}|^4 + \beta_2\,|\vec{a}\cdot\vec{a}|^2 + \beta_3\,|b|^4 + \beta_4\,|\vec{a}|^2\,|b|^2 \\ & + \tfrac{1}{4}\,\beta_5\,[\vec{a}\cdot\vec{a}\,(b^*)^2 + (\vec{a}\cdot\vec{a})^*\,b^2]. \end{aligned} \tag{3}$$

The coefficients of the second-order invariants determine the instability temperatures $T_{c_\perp}$ and $T_{c_\parallel}$ for the 2D and 1D order parameters, respectively. Thus, for temperatures $|T - T_{c_{\perp,\parallel}}| \ll T_c$ for unstrained aerogel, $\alpha_{\perp,\parallel}(T) \simeq \alpha'_{\perp,\parallel}(T - T_{c_{\perp,\parallel}})$, with $\alpha'_{\perp,\parallel} > 0$. The bare instability temperatures are equal in the isotropic limit, and thus for weak uniaxial anisotropy we assume $T_{c_\perp} - T_{c_\parallel} = \lambda\,\varepsilon_{zz}\,T_c$, where the uniaxial strain $\varepsilon_{zz} > 0$ ($\varepsilon_{zz} < 0$) for "stretched" ("compressed") aerogel, and λ is a material coefficient whose magnitude and *sign* depend on the microscopic mechanism by which anisotropy lifts the degeneracy between the 1D and 2D pairing symmetry classes.

II. NORMAL TO 2D PHASES

Consider the case in which $T_{c_\perp} > T_{c_\parallel}$. Thus, for $T \lesssim T_{c_\perp}$ there is necessarily a temperature region in which $\alpha_\perp < 0$ and $\alpha_\parallel > 0$. The GL functional in Eq. (3) is then minimized with $b \equiv 0$ and reduces to

$$\Delta\Omega[\vec{a}] = \alpha_\perp(T)\,|\vec{a}|^2 + \beta_1\,|\vec{a}|^4 + \beta_2\,|\vec{a}\cdot\vec{a}|^2. \tag{4}$$

The order parameter is a complex vector in the plane perpendicular to the strain axis ($\hat{\mathbf{z}}$), and is parametrized by

$$\vec{a} = \Delta\,(\cos\varphi\,\hat{\mathbf{x}} + e^{i\psi}\sin\varphi\,\hat{\mathbf{y}}). \tag{5}$$

Minimizing the GL functional with respect to the amplitude Δ gives

$$\Delta\Omega = \frac{1}{2}\alpha_\perp(T)\,\Delta^2 \quad \text{with} \quad \Delta^2 = -\frac{1}{2}\frac{\alpha_\perp(T)}{\beta_1 + \tilde{\beta}_2}, \tag{6}$$

where $\tilde{\beta}_2(\varphi,\psi) = \beta_2[1 - \sin^2\psi\,\sin^2(2\varphi)]$. Global stability requires $\beta_1 > 0$ and $\beta_1 + \beta_2 > 0$, however, there are two possibilities for the equilibrium phase just below $T_{c_1} \equiv T_{c_\perp}$. For $\beta_2 < 0$, the free energy is minimized for $\psi = 0, \pi$, and *any* φ, i.e., for an "in-plane" polar state,

$$\vec{a}_P = \Delta_P\,\hat{\mathbf{x}} \quad \text{with} \quad \Delta_P = \sqrt{\frac{1}{2}\frac{|\alpha_\perp(T)|}{\beta_1 + \beta_2}}. \tag{7}$$

This phase preserves time-reversal symmetry, but spontaneously breaks the $SO(2)_{L_z}$ rotational symmetry. The continuous degeneracy of the in-plane polar state under rotation of the polar axis in the plane normal to the strain axis means that this phase will be subject to the Larkin-Imry-Ma (LIM) effect, i.e., long-range orientational order of the in-plane polar order will be destroyed by random fluctuations in the anisotropy direction.[20,30,31]

For $\beta_2 > 0$, which is the prediction of weak-coupling BCS theory for weak anisotropic scattering,[12] the free energy is minimized for $\psi = \pm\pi/2$ and $\varphi = \pi/4$, i.e., by either of two degenerate *chiral* ABM states:

$$\vec{a}_{ABM} = \Delta_A\,(\hat{\mathbf{x}} \pm i\hat{\mathbf{y}})/\sqrt{2} \quad \text{with} \quad \Delta_A = \sqrt{\frac{1}{2}\frac{|\alpha_\perp(T)|}{\beta_1}}. \tag{8}$$

The ABM state breaks time-reversal symmetry, but retains continuous axial symmetry $U(1)_{L_z-N}$ by the combining each element of $SO(2)_{L_z}$ with a gauge transformation. In contrast to the ABM state in pure ^{3}He, the ABM phase stabilized by uniaxial anisotropy has its chiral axis $\hat{\mathbf{l}} = \pm\hat{\mathbf{z}}$, *locked* parallel or antiparallel to the strain axis. The absence of a continuous degeneracy associated with rotation of the chiral axis protects the ABM phase against random fluctuations in the anisotropy direction.

The geometry for the experiments reported in Ref. 19 is a cylinder of ^{3}He-aerogel with uniaxial strain $\epsilon_{zz} \simeq 0.14$, along the cylinder axis ($\hat{\mathbf{z}}$), an aspect ratio of $D/L \simeq 1.44$, and static magnetic field perpendicular to the strain axis $\mathbf{H} \simeq 0.3$–$2.0\ \text{kG}\,\hat{\mathbf{x}}$, as shown in Fig. 2. The authors identified the ESP-1 phase for this "stretched" aerogel as a chiral ABM state with chiral axis *perpendicular* to the strain axis, the easy-plane configuration shown in Fig. 2. This alignment is at odds with the GL theory presented here. A transition from the normal state to a chiral ABM state with $\hat{\mathbf{l}} \perp \hat{\mathbf{z}}$ is not allowed by symmetry. In a uniform uniaxial medium, a chiral ABM state

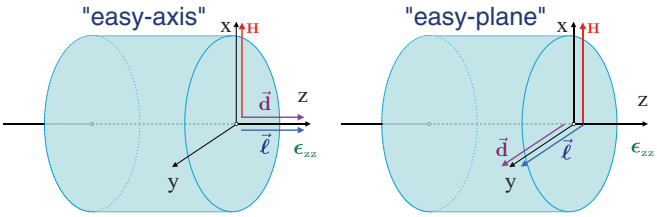

FIG. 2. (Color online) For the ABM phase confined in homogeneous uniaxial-strained aerogel, the chiral axis is aligned along the strain axis ("easy-axis" alignment) with $\hat{\mathbf{l}} \parallel \mathbf{z}$. Other models assign the chiral axis to the plane perpendicular to the strain axis ("easy-plane" alignment) with $\hat{\mathbf{l}} \perp \mathbf{z}$. Dipole-locked configurations are shown for both cases shown with the magnetic field perpendicular to the strain axis $\mathbf{H} \parallel \mathbf{x}$.

is the equilibrium phase only if the chiral axis is aligned with the strain axis, i.e., easy-axis alignment with $\hat{\mathbf{l}} = \pm\hat{\mathbf{z}}$.

The ABM state with $\hat{\mathbf{l}} \parallel \pm\hat{\mathbf{z}}$ is also at odds with the model of *strain alignment of random cylinders* combined with the alignment energy for a *single* cylindrical impurity,[20,21] which is argued to favor ABM states with $\hat{\mathbf{l}} \perp \hat{\mathbf{z}}$ for an axially stretched aerogel. To emphasize the conflict of this model with GL theory, consider an ABM order parameter in a uniform uniaxial medium, either stretched or compressed, with $\hat{\mathbf{l}} \perp \hat{\mathbf{z}}$. This requires the two orbital amplitudes that define this ABM order parameter to belong to *different* irreducible representations of the maximal symmetry group, which implies that these two amplitudes onset with *different* instability temperatures. Thus, it is not possible for an ABM state with $\hat{\mathbf{l}} \perp \hat{\mathbf{z}}$ to be the ESP-1 phase in a homogeneous uniaxial medium. In the following Sec. III, I identify the chiral ABM state with $\hat{\mathbf{l}} \parallel \pm\hat{\mathbf{z}}$ with the ESP-1 phase based on comparison between the theoretically expected NMR signatures and the NMR measurements reported in Ref. 19.

III. NMR SIGNATURES FOR THE ESP-1 PHASE

The Zeeman energy for an ESP state defined by $\vec{\mathbf{d}}$ in a magnetic field $\vec{\mathbf{H}}$ is given by[33]

$$\Delta\Omega_{\rm Z} = g_{\rm z}\,\Delta_{\rm A}(T)^2\,(\vec{\mathbf{d}}\cdot\vec{\mathbf{H}})^2, \tag{9}$$

where $g_{\rm z} > 0$.[11] Thus, the ESP state accommodates the field by orienting the $\vec{\mathbf{d}} \perp \vec{\mathbf{H}}$. The magnetization is then given by $\gamma\vec{\mathbf{S}} = \chi\vec{\mathbf{H}}$, where γ is the gyromagnetic ratio of ^{3}He and $\chi = \chi_{\rm N}$ is the ABM-phase spin susceptibility, which is unchanged from that of normal ^{3}He.[35] When a pulsed transverse rf field is applied along the strain axis $\vec{\mathbf{H}}_1 = H_1\cos(\omega t)\hat{\mathbf{z}} \perp \vec{\mathbf{H}}$, it drives the magnetization away from the static field. Leggett's equation of motion for the magnetization is

$$\partial_t\vec{\mathbf{S}} = \gamma(\vec{\mathbf{S}}\times\vec{\mathbf{H}}) + \gamma(\vec{\mathbf{S}}\times\vec{\mathbf{H}}_1) + \vec{\mathbf{R}}_{\rm D}, \tag{10}$$

where

$$\vec{\mathbf{R}}_{\rm D} = -\vec{\mathbf{d}}\times(\partial\Delta\Omega_{\rm D}/\partial\vec{\mathbf{d}}) \tag{11}$$

is the torque from the nuclear dipole energy.[4] The latter is defined by

$$\Delta\Omega_{\rm D} = g_{\rm D}\,\Delta_{\rm A}(T)^2\,[1-(\vec{\mathbf{d}}\cdot\hat{\mathbf{z}})^2] \tag{12}$$

for an axially aligned ABM state. The coupling constant $g_{\rm D} > 0$ is unrenormalized by impurity disorder,[11] and thus the dipole energy is minimized by aligning $\vec{\mathbf{d}} \parallel \hat{\mathbf{l}} \parallel \hat{\mathbf{z}}$. For time-dependent fields, the $\vec{\mathbf{d}}$ vector is driven by torque from the sum of the external and internal fields[4]

$$\partial_t\vec{\mathbf{d}} = \gamma\vec{\mathbf{d}}\times\left(\vec{\mathbf{H}} - \frac{\gamma}{\chi}\vec{\mathbf{S}} + \vec{\mathbf{H}}_1\right). \tag{13}$$

Note that for a purely static field, the steady-state condition $\gamma\vec{\mathbf{S}} = \chi\vec{\mathbf{H}}$ is consistent with the minimum of the Zeeman energy $\vec{\mathbf{d}} \perp \vec{\mathbf{H}}$. This condition is also compatible with the orientation $\vec{\mathbf{d}} \parallel \hat{\mathbf{z}}$, which minimizes the dipole energy. This is the easy-axis geometry shown in Fig. 2.

For small rf excitation, $\vec{\mathbf{S}}$ and $\vec{\mathbf{d}}$ execute small excursions about their equilibrium orientations $\vec{\mathbf{S}}_0 = S_0\hat{\mathbf{x}}$ with $\gamma S_0 = \chi H$ and $\vec{\mathbf{d}}_0 = \hat{\mathbf{z}}$, i.e., $\vec{\mathbf{S}} = \vec{\mathbf{S}}_0 + \delta\vec{\mathbf{S}}$, $\vec{\mathbf{d}} = \vec{\mathbf{d}}_0 + \delta\vec{\mathbf{d}}$ with $\vec{\mathbf{d}}_0\cdot\delta\vec{\mathbf{d}} = 0$. For the easy-axis geometry, the linearized equations of motion reduce to

$$\partial_t\delta\vec{\mathbf{S}} = \delta\vec{\mathbf{S}}\times\vec{\omega}_{\rm L} + \vec{\mathbf{S}}_0\times\vec{\omega}_1 - R_{\rm D}\,\vec{\mathbf{d}}_0\times\delta\vec{\mathbf{d}}, \tag{14}$$

$$\partial_t\delta\vec{\mathbf{d}} = -\frac{\gamma^2}{\chi}\vec{\mathbf{d}}_0\times\delta\vec{\mathbf{S}}, \tag{15}$$

with $\vec{\omega}_{\rm L} = \gamma\vec{\mathbf{H}} = \omega_{\rm L}\hat{\mathbf{x}}$, $\vec{\omega}_1 = \gamma\vec{\mathbf{H}}_1 = \omega_1(t)\hat{\mathbf{z}}$, and $R_{\rm D} = 2g_{\rm D}\,\Delta_{\rm A}(T)^2$. The latter determines the longitudinal resonance frequency for the ABM phase $\Omega_{\rm A}^2 = \gamma^2\,R_{\rm D}/\chi$. For the easy-axis geometry with the rf field along the strain axis the only components that are excited by the rf field are $\delta d_x, \delta S_y$, and δS_z. For a single Fourier component of frequency ω, the coupled Leggett equations are

$$\begin{pmatrix} \omega & -i\Omega_{\rm A} & 0 \\ +i\Omega_{\rm A} & \omega & -i\omega_{\rm L} \\ 0 & +i\omega_{\rm L} & \omega \end{pmatrix}\begin{pmatrix} \delta D_x \\ \delta S_y \\ \delta S_z \end{pmatrix} = \begin{pmatrix} 0 \\ -iS_0\,\omega_1 \\ 0 \end{pmatrix}, \tag{16}$$

with $\delta D_x \equiv (R_{\rm D}/\Omega_{\rm A})\delta d_x$. The retarded linear response functions are then given by

$$\begin{pmatrix} \delta D_x \\ \delta S_y \\ \delta S_z \end{pmatrix} = \frac{S_0\,\omega_1}{(\omega+i\eta)^2 - \left(\omega_{\rm L}^2+\Omega_{\rm A}^2\right)}\begin{pmatrix} +\Omega_{\rm A} \\ -i\omega \\ -\omega_{\rm L} \end{pmatrix}, \tag{17}$$

with $\eta \to 0+$, which exhibit transverse NMR at $\omega = \sqrt{\omega_{\rm L}^2+\Omega_{\rm A}^2}$, and thus a maximum NMR frequency shift in the high-field limit $\omega_{\rm L} \gg \Omega_{\rm A}$:

$$\Delta\omega = \omega - \omega_{\rm L} \simeq \tfrac{1}{2}\Omega_{\rm A}^2/\omega_{\rm L}. \tag{18}$$

For finite tipping angle, defined by $\vec{\mathbf{S}}(t=0+) = S_0(\cos\beta\hat{\mathbf{x}} + \sin\beta\hat{\mathbf{z}})$, this result extends to the known result for the dipole-locked A phase[36]

$$\Delta\omega = \tfrac{1}{2}\Omega_{\rm A}^2/\omega_{\rm L}\left(\tfrac{1}{4}+\tfrac{3}{4}\cos\beta\right). \tag{19}$$

These results for the easy-axis geometry agree quantitatively with experimental results for the ESP-1 phase in axially stretched aerogel reported in Ref. 19, and thus the ESP-1 phase is identified as the *ABM state with chiral axis* $\hat{\mathbf{l}}$ *aligned along the strain axis*.

A test of this identification can be made by reorienting the "stretched" ^{3}He-aerogel sample with the static field aligned along the strain axis, i.e., $\vec{\mathbf{H}} = H\hat{\mathbf{z}}$. In the high-field limit $\omega_{\rm L} \gg \Omega_{\rm A}$, this is a *dipole-unlocked* configuration with $\vec{\mathbf{d}}_0 \perp \vec{\mathbf{H}} \rightsquigarrow \vec{\mathbf{d}}_0 \perp \hat{\mathbf{l}}$, e.g., $\vec{\mathbf{d}}_0 = \hat{\mathbf{y}}$ located at a maximum of the dipole potential. Under rf excitation with $\vec{\omega}_1 \parallel \hat{\mathbf{x}}$ for small tipping angles, the dipole torque is $\vec{\mathbf{R}}_{\rm D} = R_{\rm D}\,\delta d_z\,\hat{\mathbf{x}}$. The Leggett equations couple $\delta S_x, \delta S_y$, and $\delta D_z = (R_{\rm D}/\Omega_{\rm A})\delta d_z$, and lead to the response functions

$$\begin{pmatrix} \delta S_x \\ \delta S_y \\ \delta D_z \end{pmatrix} \simeq \frac{S_0\,\omega_1}{(\omega+i\eta)^2 - \left(\omega_{\rm L}^2-\Omega_{\rm A}^2\right)}\begin{pmatrix} -\omega_{\rm L} \\ i\omega \\ -i\omega(\Omega_{\rm A}/\omega_{\rm L}) \end{pmatrix}, \tag{20}$$

exhibiting a *negative* frequency shift of the NMR resonance

$$\Delta\omega \simeq -\tfrac{1}{2}\Omega_{\rm A}^2/\omega_{\rm L}. \tag{21}$$

By contrast, for the easy-plane configuration of the chiral axis proposed in Ref. 19, *both* field orientations yield a

positive frequency shift of $\Delta\omega \simeq +\frac{1}{2}\Omega_A^2/\omega_L$. Thus, these two orientations of the NMR field provide a stringent test of the identification of the ESP-1 order parameter, and in particular this GL theory of ESP pairing in a uniformly anisotropic medium.

IV. INTERLUDE: NORMAL TO 1D TRANSITION

Given that the onset of superfluidity in homogeneously anisotropic "stretched" aerogel reported in Ref. 19 is well described by a normal to 2D transition ($T_{c_\perp} > T_{c_\parallel}$) into the axially aligned ABM state, this theory predicts for the case $T_{c_\parallel} > T_{c_\perp}$ a normal to 1D transition. In particular, the GL functional for $T \lesssim T_{c_1} \equiv T_{c_\parallel}$ is minimized by $\vec{a} \equiv 0$, and reduces to

$$\Delta\Omega[b] = \alpha_\parallel(T)\,|b|^2 + \beta_3\,|b|^4. \tag{22}$$

The resulting equilibrium phase is an ESP state with an axially aligned polar order parameter

$$\vec{b}_P = b\hat{\mathbf{z}} \quad \text{with} \quad b = \sqrt{\frac{1}{2}\,\frac{|\alpha_\parallel(T)|}{\beta_3}}. \tag{23}$$

Global stability requires $\beta_3 > 0$.

The dipole potential for the ESP polar phase is

$$\Delta\Omega_D = 2\,g_D\,b(T)^2\,(\vec{\mathbf{d}}\cdot\hat{\mathbf{z}})^2. \tag{24}$$

Thus, in contrast to the axially aligned ABM state, $\vec{\mathbf{d}} \perp \hat{\mathbf{z}}$ in equilibrium for the strain aligned polar phase. For any other orientation of $\vec{\mathbf{d}}$, the dipole torque is given by

$$\vec{\mathbf{R}}_D = -4\,g_D\,b(T)^2\,(\vec{\mathbf{d}}\cdot\hat{\mathbf{z}})(\vec{\mathbf{d}}\times\hat{\mathbf{z}}). \tag{25}$$

The corresponding longitudinal resonance frequency for the polar phase is $\Omega_P^2 = (\gamma^2/\chi)\,4g_D\,b(T)^2$. Note that the ratio of the slopes of the square of the longitudinal frequencies for the ABM and polar phases is given by

$$\frac{\partial\Omega_P^2/\partial T|_{T_c}}{\partial\Omega_A^2/\partial T|_{T_c}} = 2\frac{\alpha'_\parallel}{\alpha'_\perp}\frac{\beta_1}{\beta_3}. \tag{26}$$

The Zeeman energy for the polar phase

$$\Delta\Omega_Z = g_z\,b(T)^2\,(\vec{\mathbf{d}}\cdot\vec{\mathbf{H}})^2 \tag{27}$$

is minimized by $\vec{\mathbf{d}} \perp \vec{\mathbf{H}}$. Thus, for $\mathbf{H} \parallel \hat{\mathbf{x}}$ both the dipole energy and Zeeman energy are are minimized for $\vec{\mathbf{d}} \parallel \hat{\mathbf{y}}$. Transverse rf excitation with $\vec{\mathbf{H}}_1 \parallel \hat{\mathbf{z}}$ gives a transverse NMR resonance at $\omega = \omega_L$, i.e., "zero shift." However, if we reorient the static field along the compression axis and the rf field transverse, e.g., $\vec{\mathbf{H}}_1 \parallel \hat{\mathbf{x}}$, then we obtain positive NMR shift of $\Delta\omega = \frac{1}{2}\Omega_P^2/\omega_L$ in the high-field limit. Note that the polar phase is also protected by the anisotropy energy from random fluctuations of the anisotropy axis, and thus expected to exhibit a sharp NMR line for both orientations.

Recently, ^{3}He has been infused into a new type of high-porosity aerogel formed from long strands of aluminum oxide, so-called "nematic aerogels," exhibiting strong uniaxial anisotropy.[37] ^{3}He NMR measurements indicate that the onset of superfluidity in this medium is to a 1D polar phase.[38] If this interpretation is correct, then this may be the first observation of a 1D polar phase in superfluid ^{3}He. Added support for this interpretation is included in Sec. VIII.

V. SECOND ESP PHASE

Returning to the normal to 2D case ($T_{c_\perp} > T_{c_\parallel}$), for weak uniaxial anisotropy a second phase transition is predicted. The "bare" instability temperature $T_{c_\parallel}$ is renormalized by the 2D order parameter that develops below $T_{c_\perp}$. Whether or not a second transition occurs depends on the magnitude of $T_{c_\perp} - T_{c_\parallel}$ and the sign of the interaction terms coupling the 2D and 1D order parameters. In particular, a second transition exists if the coefficient of the quadratic term for the 1D polar phase vanishes at T_{c_2}. For the case in which the axially aligned ABM state [Eq. (8)] is the equilibrium state for $T_{c_2} \leqslant T < T_{c_1}$, the terms proportional to β_5 in Eq. (3) vanish at T_{c_2}, in which case the second-order term in the GL functional for $T \to T_{c_2}$ is given by

$$\Delta\Omega[\vec{a}_A, b] = \Delta\Omega_A(T) + \tilde{\alpha}_\parallel(T)\,|b|^2 + \mathcal{O}(b^4), \tag{28}$$

with

$$\tilde{\alpha}_\parallel(T) = \alpha_\parallel(T) + \beta_4\,\Delta_A(T)^2, \tag{29}$$

where $\Delta\Omega_A(T) = \frac{1}{2}\alpha_\perp(T)\,\Delta_A^2(T)$ is the free energy of the ABM phase. Thus, a second-order instability to a mixed symmetry phase with $b \neq 0$ occurs for $\tilde{\alpha}_\parallel(T_{c_2}) = 0$, which gives

$$T_{c_2} - T_{c_1} = \left(\frac{\alpha'_\parallel}{\alpha'_\parallel - \alpha'_\perp\,\beta_4/2\beta_1}\right)(T_{c_\parallel} - T_{c_\perp}). \tag{30}$$

For $\beta_4/\beta_1 > 0$, we have $T_{c_2} < T_{c_\parallel}$, but the transition is not suppressed to zero temperature, at least within GL theory.

Below T_{c_2} the full GL functional in Eq. (3) must be minimized, including the β_5 terms since the 2D order parameter need not remain a purely axial ABM phase. Indeed, one expects the 2D order parameter to be deformed from a pure ABM state due to the interaction terms. It is convenient to parametrize the 2D order parameter below T_{c_2} in terms of the chiral basis vectors $\hat{\mathbf{x}}_\pm = \frac{1}{\sqrt{2}}\,(\hat{\mathbf{x}} \pm i\hat{\mathbf{y}})$:

$$\vec{a} = a_+\,\hat{\mathbf{x}}_+ + a_-\,\hat{\mathbf{x}}_-. \tag{31}$$

Note that $\hat{\mathbf{x}}_\pm \cdot \hat{\mathbf{x}}_\pm^* = 1$, $\hat{\mathbf{x}}_\pm \cdot \hat{\mathbf{x}}_\pm = 0$, and $\hat{\mathbf{x}}_+ \cdot \hat{\mathbf{x}}_- = 1$. It is also useful to introduce amplitude and phase variables for each order parameter

$$a_\pm = \Delta_\pm\,e^{i\alpha_\pm}, \quad b = \Delta_z\,e^{i\beta}. \tag{32}$$

The GL functional can be conveniently expressed in terms of $u = \Delta_+^2$, $v = \Delta_-^2$, $w = \Delta_z^2$, and the relative phase variable $\Phi = \alpha_+ + \alpha_- - 2\beta$:

$$\begin{aligned}\Delta\Omega[u,v,w,\Phi] = {}& \alpha_\perp(u+v) + \beta_1(u+v)^2 + \beta_2\,4\,u\,v \\ & + \alpha_\parallel\,w + \beta_3\,w^2 + \beta_4(u+v)\,w \\ & + \beta_5\sqrt{u}\sqrt{v}\,w\,\cos\Phi.\end{aligned} \tag{33}$$

The stationarity conditions with respect to u, v, w, and Φ are

$$\begin{aligned}\frac{\partial\Delta\Omega}{\partial u} = {}& \alpha_\perp + 2\beta_1(u+v) + 4\beta_2\,v + \beta_4\,w \\ & + \frac{1}{2}\beta_5\sqrt{\frac{v}{u}}\,w\,\cos\Phi = 0,\end{aligned} \tag{34}$$

$$\frac{\partial \Delta\Omega}{\partial v} = \alpha_\perp + 2\beta_1(u+v) + 4\beta_2\, u + \beta_4\, w + \frac{1}{2}\beta_5\sqrt{\frac{u}{v}}\, w\, \cos\Phi = 0, \tag{35}$$

$$\frac{\partial \Delta\Omega}{\partial w} = \alpha_\parallel + 2\beta_3 w + \beta_4\,(u+v) + \beta_4\, w + \beta_5\sqrt{u}\sqrt{v}\, \cos\Phi = 0, \tag{36}$$

$$\frac{\partial \Delta\Omega}{\partial \Phi} = -\beta_5\sqrt{u}\sqrt{v}\, w\, \sin\Phi = 0. \tag{37}$$

For $T < T_{c_2}$, we have $u \neq 0$ with both v and w growing continuously from zero at T_{c_2}. The difference of Eqs. (34) and (35) yields

$$(v-u)\left\{4\beta_2 + \frac{1}{2}\beta_5\frac{w}{\sqrt{uv}}\cos\Phi\right\} = 0, \tag{38}$$

and since $v - u \neq 0$ and $w \neq 0$ for $T < T_{c_2}$, we obtain

$$\sqrt{uv} = -\frac{1}{8}\frac{\beta_5}{\beta_2}\, w\, \cos\Phi. \tag{39}$$

This equation constrains the range of $\cos\Phi$: (i) $-1 \leqslant \cos\Phi < 0$ for $\beta_5 > 0$, while (ii) $0 < \cos\Phi \leqslant 1$ for $\beta_5 < 0$. Equation (37) then fixes $\cos\Phi = \pm 1$ depending on the sign of β_5. The sum of Eqs. (34) and (35), combined with Eq. (39), gives

$$u + v = -\frac{\alpha_\perp}{2\beta_1} - \frac{\beta_4}{2\beta_1}\, w, \tag{40}$$

which is used to obtain the free-energy functional for the polar condensate density w for $T < T_{c_2}$:

$$\Delta\Omega[w] = \Delta\Omega_{\rm A}(T) + \tilde{\alpha}_\parallel(T)\, w + \beta_{\rm w}(\Phi)\, w^2, \tag{41}$$

where

$$\tilde{\alpha}_\parallel(T) = \alpha_\parallel(T) - \frac{1}{2}\frac{\beta_4}{\beta_1}\alpha_\perp(T), \tag{42}$$

$$\beta_{\rm w}(\Phi) = \beta_3 - \frac{1}{4}\frac{\beta_4^2}{\beta_1} - \frac{1}{8}\frac{\beta_5^2}{\beta_2}\cos^2\Phi. \tag{43}$$

A second transition develops when $\tilde{\alpha}_\parallel(T_{c_2}) = 0$, which is the instability temperature given in Eq. (30). Below T_{c_2}, the polar phase density is given by

$$w(T) = -\frac{\tilde{\alpha}_\parallel}{2\beta_{\rm w}(\Phi)}, \tag{44}$$

and a reduced thermodynamic potential given by

$$\Delta\Omega(T) = -\frac{1}{4}\frac{\alpha_\perp^2}{\beta_1} - \frac{1}{4}\frac{\tilde{\alpha}_\parallel^2}{\beta_{\rm w}(\Phi)}, \quad T < T_{c_2}. \tag{45}$$

The ordered state for $T < T_{c_2}$ with the lowest free energy is given by the smallest allowed positive value of $\tilde{\beta}_{\rm w}(\Phi)$, which fixes the internal phase to be $\cos\Phi = +1$ for $\beta_5 < 0$ or $\cos\Phi = -1$ for $\beta_5 > 0$.

The orbital order parameter, above and below T_{c_2}, can be expressed in the form

$$\vec{a}_{\rm A} = \Delta_{\rm A}(T)\,\hat{\mathbf{x}}_+, \quad T_{c_2} < T < T_{c_1} \tag{46}$$

where I have assigned the phase $\alpha_+ = 0$ for the axially aligned ABM phase. The order parameter for the low-temperature mixed-symmetry phase then takes the form

$$\vec{\mathscr{A}} = \Delta_+(T)\,\hat{\mathbf{x}}_+ + e^{i\alpha_-}\Delta_-(T)\,\hat{\mathbf{x}}_- + e^{i\beta}\Delta_z(T)\,\hat{\mathbf{z}}, \quad T < T_{c_2} \tag{47}$$

where the order-parameter amplitudes are given by

$$\Delta_{\rm A}(T) = \bar{\Delta}_{\rm A}\sqrt{1 - T/T_{c_1}}, \quad T \leqslant T_{c_1} \tag{48}$$

$$\bar{\Delta}_{\rm A} = \sqrt{\frac{T_{c_1}}{2\beta_1}\frac{d\alpha_\perp}{dT}\bigg|_{T_{c_1}}} \tag{49}$$

for the axially aligned ABM phase above T_{c_2} (ESP-1). For the low-temperature phase, the polar amplitude is given by

$$\Delta_z = \bar{\Delta}_z\sqrt{1 - T/T_{c_2}}, \quad T \leqslant T_{c_2} \tag{50}$$

$$\bar{\Delta}_z = \sqrt{\frac{T_{c_2}}{2\beta_1}\frac{d\tilde{\alpha}_\parallel}{dT}\bigg|_{T_{c_2}}\frac{1}{\bar{\beta}_{\rm w}}}, \tag{51}$$

with

$$\bar{\beta}_{\rm w} = \bar{\beta}_3 - \tfrac{1}{4}\,\bar{\beta}_4^2 - \tfrac{1}{8}\,\bar{\beta}_5^2/\bar{\beta}_2. \tag{52}$$

Note the dimensionless β parameters are normalized by β_1: $\bar{\beta}_i = \beta_i/\beta_1$. For $T < T_{c_2}$, we can express the two chiral amplitudes $\Delta_\pm(T)$ in terms of $\Delta_z(T)$ and Eq. (48) for $\Delta_{\rm A}(T)$, extended to $T < T_{c_2}$, as follows:

$$\Delta_\pm = \frac{1}{2}(\Delta_s \pm \Delta_d), \tag{53}$$

$$\Delta_s = \sqrt{\Delta_{\rm A}^2(T) - \frac{1}{2}\left(\bar{\beta}_4 - \frac{1}{2}\bar{\beta}_5/\bar{\beta}_2\right)\Delta_z^2(T)}, \tag{54}$$

$$\Delta_d = \sqrt{\Delta_{\rm A}^2(T) - \frac{1}{2}\left(\bar{\beta}_4 + \frac{1}{2}\bar{\beta}_5/\bar{\beta}_2\right)\Delta_z^2(T)}. \tag{55}$$

A. Biaxial and chiral order

The low-temperature ESP phase has a continuous degeneracy associated with the *relative* phases of the polar (β) and ABM amplitudes ($\alpha_\pm$) defining the mixed-symmetry order parameter in Eq. (47). For $\bar{\beta}_5 > 0$, the constraint $\alpha_+ + \alpha_- - 2\beta = \pi$ allows us to parametrize the internal degeneracy by a single phase angle on the interval $0 \leqslant \varphi \leqslant 2\pi$, and express the mixed-symmetry order parameter as

$$\vec{\mathscr{A}} = \Delta_+(T)\, e^{-i\varphi}\,\hat{\mathbf{x}}_+ - \Delta_-(T)\, e^{+i\varphi}\,\hat{\mathbf{x}}_- + \Delta_z(T)\,\hat{\mathbf{z}}, \tag{56}$$

up to an overall phase. Note that the chiral basis vectors transform under gauge transformations as

$$e^{\mp i\varphi}\,\hat{\mathbf{x}}_\pm = \hat{\mathbf{x}}'_\pm = (\hat{\mathbf{x}}' \pm i\hat{\mathbf{y}}')/\sqrt{2}, \tag{57}$$

where $\hat{\mathbf{x}}' = \cos\varphi\,\hat{\mathbf{x}} + \sin\varphi\,\hat{\mathbf{y}}$ and $\hat{\mathbf{y}}' = -\sin\varphi\,\hat{\mathbf{x}} + \cos\varphi\,\hat{\mathbf{y}}$ are rotations of the in-plane orbital axes $(\hat{\mathbf{x}},\hat{\mathbf{y}})$ about the strain axis $\hat{\mathbf{z}}$. This implies that the continuous degeneracy associated with the internal phase φ corresponds to *spontaneous breaking of the axial symmetry* of the ABM phase at T_{c_2}.

Further insight is obtained by considering the product $\mathscr{A}_i\,\mathscr{A}_j^*$. This tensor determines observables such as the the momentum-dependent "gap function" $\Delta(\hat{\mathbf{p}})$, the superfluid density tensor $(\rho_s)_{ij}$, the nuclear dipole-dipole energy $\Delta\Omega_{\rm D}$, the intrinsic angular momentum density $\vec{\mathscr{L}}$, etc. The tensor $\mathscr{A}_i\,\mathscr{A}_j^* = \Delta_{ij} + \mathscr{L}_{ij}$ separates into a real symmetric tensor

Δ_{ij}, and an imaginary, antisymmetric tensor $\mathscr{L}_{ij}$. The real order-parameter tensor is given by

$$\Delta_{ij} = \frac{1}{2}(\Delta_+^2 + \Delta_-^2)\,(\hat{\mathbf{x}}_i\hat{\mathbf{x}}_j + \hat{\mathbf{y}}_i\hat{\mathbf{y}}_j) + \Delta_z^2\,\hat{\mathbf{z}}_i\hat{\mathbf{z}}_j - \Delta_+\Delta_-\,(\hat{\mathbf{x}}_i\hat{\mathbf{x}}_j - \hat{\mathbf{y}}_i\hat{\mathbf{y}}_j) + \frac{1}{\sqrt{2}}\,\Delta_z(\Delta_+ - \Delta_-)\,(\hat{\mathbf{x}}_i\hat{\mathbf{z}}_j + \hat{\mathbf{z}}_i\hat{\mathbf{x}}_j). \tag{58}$$

The first line of terms in Eq. (58), which preserve axial symmetry, includes the polar distortion $\sim\hat{\mathbf{z}}_i\hat{\mathbf{z}}_j$ that varies as $\Delta_z^2 \sim (1 - T/T_{c_2})$ below T_{c_2}. However, the second line $\sim(\hat{\mathbf{x}}_i\hat{\mathbf{x}}_j - \hat{\mathbf{y}}_i\hat{\mathbf{y}}_j)$ exhibits the spontaneously broken axial symmetry of the ESP-2 phase. Thus, the ESP-2 phase possesses *biaxial anisotropy* with a magnitude scaling as $\Delta_+\Delta_- \sim (1 - T/T_{c_2})$ below T_{c_2}. The polar and in-plane distortions conspire to generate the biaxial anisotropy represented by $\sim(\hat{\mathbf{x}}_i\hat{\mathbf{z}}_j + \hat{\mathbf{z}}_i\hat{\mathbf{x}}_j)$, which scales as $\Delta_z(\Delta_+ - \Delta_-) \sim (1 - T/T_{c_2})^{\frac{1}{2}}$ below T_{c_2}. The biaxial anisotropy of the ESP-2 phase can be expressed in terms of semimajor $\Delta_s\hat{\mathbf{y}}$ and semiminor $\Delta_d\hat{\mathbf{x}}$ axes defining the in-plane gap distortion by combining the terms using Eqs. (53)–(55). The continuous degeneracy of the biaxial phase corresponds to the orientation of the semimajor and semiminor axes in the plane perpendicular to the strain axis $\hat{\mathbf{z}}$. Since Δ_{ij} is real and symmetric, it can be expressed in diagonal form in terms of tensor products of an orthonormal triad $\{\hat{\mathbf{m}},\hat{\mathbf{n}},\hat{\mathbf{l}}\}$ that can be expressed as a rotation of the laboratory axes $\{\hat{\mathbf{x}},\hat{\mathbf{y}},\hat{\mathbf{z}}\}$ as follows:

$$\hat{\mathbf{m}} = +\cos\vartheta(\cos\varphi\,\hat{\mathbf{x}} + \sin\varphi\,\hat{\mathbf{y}}) + \sin\vartheta\,\hat{\mathbf{z}}, \tag{59}$$

$$\hat{\mathbf{n}} = -\sin\varphi\,\hat{\mathbf{x}} + \cos\varphi\,\hat{\mathbf{y}}, \tag{60}$$

$$\hat{\mathbf{l}} = -\sin\vartheta(\cos\varphi\,\hat{\mathbf{x}} + \sin\varphi\,\hat{\mathbf{y}}) + \cos\vartheta\,\hat{\mathbf{z}}, \tag{61}$$

where $0 \leqslant \varphi \leqslant 2\pi$ is the in-plane gauge-rotation angle defined in Eq. (56) that parametrizes the degeneracy of the biaxial phase, while the polar rotation ϑ is fixed by energetics

$$\cos\vartheta = \Delta_d/\sqrt{\Delta_d^2 + 2\Delta_z^2}, \quad \sin\vartheta = \sqrt{2}\Delta_z/\sqrt{\Delta_d^2 + 2\Delta_z^2}. \tag{62}$$

The resulting biaxial tensor order parameter reduces to

$$\Delta_{ij} = \tfrac{1}{2}\left(\Delta_d^2 + 2\Delta_z^2\right)\hat{\mathbf{m}}_i\hat{\mathbf{m}}_j + \tfrac{1}{2}\,\Delta_s^2\,\hat{\mathbf{n}}_i\hat{\mathbf{n}}_j. \tag{63}$$

The zero eigenvalue associated with the eigenvector $\hat{\mathbf{l}}$ means that $\pm\hat{\mathbf{l}}$ are *nodal directions* of the momentum-space pair amplitude $|\Delta(\hat{\mathbf{p}})| = (\hat{p}_i\,\Delta_{ij}\,\hat{p}_j)^{\frac{1}{2}}$. Thus, the nodal points associated with the ABM state (ESP-1 phase) are not destroyed by the second-order transition to the biaxial ESP-2 phase, but *rotate* from the points $\pm\hat{\mathbf{z}}$ (corresponding to momenta along the strain axis) to the points $\pm\hat{\mathbf{l}}$. This rotation of the point nodes off the $\hat{\mathbf{z}}$ axis leads directly to the continuous degeneracy of the biaxial phase characterized by the *orientation* of the nodal points in the plane perpendicular to the strain axis as shown in Fig. 3. Thus, $\hat{\mathbf{l}}$ defines the spontaneously broken axis appearing below T_{c_2}, whose degeneracy is parametrized by the gauge-rotation angle φ.

Furthermore, the nodal directions reflect the *chiral* nature of the biaxial phase. This is revealed by the antisymmetric

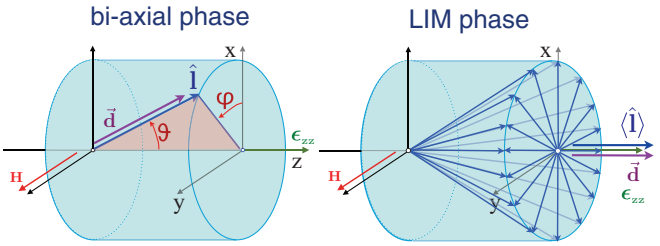

FIG. 3. (Color online) Left: The biaxial phase in uniaxially stretched aerogel is represented by the chiral axis $\hat{\mathbf{l}}$, which can lie on a cone with angle ϑ relative to the strain axis $\hat{\mathbf{z}}$. The dipole energy is minimized by $\vec{\mathbf{d}} \parallel \pm\hat{\mathbf{l}}$. Right: For the disordered biaxial LIM phase, the chiral axis is distributed on the "degeneracy cone." The average dipole energy is minimized for $\vec{\mathbf{d}} \parallel \pm\langle\hat{\mathbf{l}}\rangle$, where $\langle\hat{\mathbf{l}}\rangle = \langle\mathbf{l}\rangle\,\hat{\mathbf{z}}$ is the LIM-averaged chiral order parameter.

order-parameter tensor $\mathscr{L}_{ij}$, which can be expressed as

$$\mathscr{L}_{ij} = -\frac{i}{2}\,\Delta_s\Delta_d\,\varepsilon_{ijk}\,\hat{\mathbf{z}}_k + \frac{i}{2}\sqrt{2}\Delta_z\Delta_s\,\varepsilon_{ijk}\,\hat{\mathbf{x}}_k. \tag{64}$$

For $T > T_{c_2}$, $\mathscr{L}_{ij} \to \frac{-i}{2}\Delta_{\rm A}\,\varepsilon_{ijk}\hat{\mathbf{z}}_k$, which is directly related to the *intrinsic angular momentum density* $\vec{\mathscr{L}}_{\rm A} = \kappa_a(4m/\hbar)\Delta_{\rm A}^2\,\hat{\mathbf{z}}$ for a condensate of Cooper pairs each with orbital angular momentum $+\hbar$ along $\hat{\mathbf{z}}$.[4,39–41] Below T_{c_2}, $\mathscr{L}_{ij}$ can also be expressed in terms of a single chiral axis

$$\mathscr{L}_{ij} = -\frac{i}{2}\,\Delta_s\sqrt{\Delta_d^2 + 2\Delta_z^2}\,\varepsilon_{ijk}\,\hat{\mathbf{l}}_k \tag{65}$$

generating the nodal directions along $\pm\hat{\mathbf{l}}$, and an intrinsic angular momentum density in the biaxial phase given by

$$\vec{\mathscr{L}} = \kappa_a(4m/\hbar)\Delta_s\sqrt{\Delta_d^2 + 2\Delta_z^2}\,\hat{\mathbf{l}}. \tag{66}$$

The GL material coefficient κ_a was calculated by Choi and Muzikar.[41] For pure ^{3}He, the resulting intrinsic angular momentum density is exceedingly small, $\mathscr{L} \sim n[\Delta(T)/E_f]^2\hbar$, where n is the ^{3}He density. However, impurity disorder leads to larger orbital currents, reflected in $\kappa_a \sim (n/E_f)\,\xi_0^2\,(\xi_0/\bar{\ell})$ where $\xi_0 = \hbar v_f/2\pi T_c$ is the Cooper-pair size and $\bar{\ell}$ is the transport mean-free path resulting from scattering by impurities. This leads to an intrinsic angular momentum density of order $\mathscr{L} \sim n\hbar(\xi_0/\bar{\ell})[\Delta(T)/2\pi T_c]^2$.[41] Experimental observation of the intrinsic angular momentum density would provide a direct signature of *chiral order* predicted for both ESP phases discussed here for ^{3}He in uniaxially stretched aerogel.

VI. NMR SIGNATURES OF THE ESP-2 PHASE

The recent report of the discovery of two *chiral* superfluid phases of ^{3}He in uniaxially stretched areogel[19] is based on their NMR signatures. The identification of the ESP-1 as the axially aligned ABM phase was discussed in Sec. III. The authors of Ref. 19 tentatively identified the ESP-2 phase s a *textural transition* of an easy-plane ABM state. However, the theory presented here demonstrates that this identification is *not* allowed by symmetry for superfluid ^{3}He infused into a *uniformly anisotropic* aerogel.

Here, I calculate the NMR signatures of the biaxial phase predicted for $T \leqslant T_{c_2}$, and compare with the observed NMR

spectra for the low-temperature (ESP-2) phase. This leads to the identification of the ESP-2 phase as a "biaxial LIM phase" resulting from orientational disorder induced by the random potential, i.e., the Larkin-Imry-Ma (LIM) effect,[30,31] discussed in the context of ^{3}He-aerogel by Volovik.[20,42] First consider the spin dynamics for a *homogeneous* biaxial phase.

The Zeeman energy takes the same form as Eq. (9) for the axially aligned ABM

$$\Delta\Omega_{\rm Z} = g_z\,\Delta_{\rm B}(T)^2\,(\vec{\mathbf{d}}\cdot\vec{\mathbf{H}})^2, \tag{67}$$

but with the order-parameter amplitude

$$\Delta_{\rm B}^2 = \Delta_{\rm A}^2 + \left(1-\tfrac{1}{2}\bar\beta_4\right)\Delta_z^2. \tag{68}$$

The nuclear dipolar potential $\Delta\Omega_{\rm D} = 2g_{\rm D}\,\mathbf{d}_i\,\Delta_{ij}\,\mathbf{d}_j$ is simply expressed in the basis of biaxial eigenvectors $\{\hat{\mathbf{m}},\hat{\mathbf{n}},\hat{\mathbf{l}}\}$:

$$\Delta\Omega_{\rm D} = g_{\rm D}\,\left(\Delta_d^2+2\Delta_z^2\right)(\hat{\mathbf{m}}\cdot\vec{\mathbf{d}})^2 + g_{\rm D}\,\Delta_s^2\,(\hat{\mathbf{n}}\cdot\vec{\mathbf{d}})^2. \tag{69}$$

The dipole energy is minimized by orienting $\vec{\mathbf{d}}$ parallel to the chiral axis $\hat{\mathbf{l}}$, the latter of which is degenerate in orientation on a cone centered about the $\hat{\mathbf{z}}$ axis defined by angle ϑ as shown in Fig. 3. For the homogeneous biaxial phase, the Zeeman energy resolves the continuous degeneracy by orienting the dipole-locked biaxial state with $\vec{\mathbf{d}}\parallel\hat{\mathbf{l}}\perp\vec{\mathbf{H}}$, i.e., $\varphi=0,\pi$. For any other orientation of $\vec{\mathbf{d}}$, the dipole torque is given by

$$\vec{\mathbf{R}}_{\rm D} = -2g_{\rm D}\big[\left(\Delta_d^2+2\Delta_z^2\right)(\vec{\mathbf{d}}\cdot\hat{\mathbf{m}})\vec{\mathbf{d}}\times\hat{\mathbf{m}} + \Delta_s^2(\vec{\mathbf{d}}\cdot\hat{\mathbf{n}})\vec{\mathbf{d}}\times\hat{\mathbf{n}}\big]. \tag{70}$$

The linearized Leggett equations are of the same form as Eqs. (10) and (13), but with $\vec{\mathbf{d}}_0=\hat{\mathbf{l}}$ and $\vec{\mathbf{R}}_{\rm D}$ given by

$$\vec{\mathbf{R}}_{\rm D} = \overleftrightarrow{\mathbf{R}}_{\rm D}\cdot(\vec{\mathbf{d}}_0\times\delta\vec{\mathbf{d}}), \tag{71}$$

where

$$\overleftrightarrow{\mathbf{R}}_{\rm D} = -R_s(\hat{\mathbf{m}}\hat{\mathbf{m}}+\hat{\mathbf{l}}\hat{\mathbf{l}}) - R_d\,\hat{\mathbf{n}}\hat{\mathbf{n}}, \tag{72}$$

$R_s = 2g_{\rm D}\Delta_s^2$, and $R_d = 2g_{\rm D}(\Delta_d^2+2\Delta_z^2)$.

For the geometry in Fig. 3, $\gamma\vec{\mathbf{S}}_0=\chi\mathbf{H}$, $\vec{\omega}_{\rm L}=\gamma\vec{\mathbf{H}}=\omega_{\rm L}\hat{\mathbf{y}}$, and $\vec{\omega}_1=\gamma\vec{\mathbf{H}}_1$, and for the dipole-locked biaxial state with $\vec{\mathbf{d}}_0=\hat{\mathbf{l}}\perp\vec{\mathbf{H}}$, the chiral axis is confined in the x-z plane, and the biaxial triad can be expressed in the NMR coordinates: $\hat{\mathbf{m}}\equiv\hat{\mathbf{x}}'=\cos\vartheta\,\hat{\mathbf{x}}-\sin\vartheta\,\hat{\mathbf{z}}$, $\hat{\mathbf{n}}=\hat{\mathbf{y}}$, and $\hat{\mathbf{l}}\equiv\hat{\mathbf{z}}'=\cos\vartheta\,\hat{\mathbf{z}}+\sin\vartheta\,\hat{\mathbf{x}}$. In this basis, the linearized equations separate into a pair of equations, for the longitudinal response,

$$\begin{pmatrix}\delta D_{x'}\\ \delta S_y\end{pmatrix} = -\frac{(-iR_d/\Omega_d)(\hat{\mathbf{y}}\cdot\vec{\omega}_1)}{(\omega+i\eta)^2-\Omega_d^2}\begin{pmatrix}\omega\\ -i\Omega_d\end{pmatrix} \tag{73}$$

with $\delta D_{x'}\equiv R_d\delta\mathbf{d}_{x'}/\Omega_d$ and

$$\Omega_d^2 \equiv \frac{\gamma^2}{\chi}\,2g_{\rm D}\left(\Delta_d^2+2\Delta_z^2\right). \tag{74}$$

The pole at $\omega=\Omega_d$ is the longitudinal NMR resonance frequency, which is excited only if $\hat{\mathbf{y}}\cdot\vec{\omega}_1\neq 0$. The transverse spin response functions are given by

$$\begin{pmatrix}\delta S_{x'}\\ \delta D_y\\ \delta S_{z'}\end{pmatrix} = \frac{\chi/\gamma^2}{(\omega+i\eta)^2-\left(\omega_{\rm L}^2+\Omega_s^2\right)} \times\begin{pmatrix}+i\omega\omega_{\rm L}(\hat{\mathbf{z}}'\cdot\vec{\omega}_1)-\left(\omega_{\rm L}^2+\Omega_s^2\right)(\hat{\mathbf{x}}'\cdot\vec{\omega}_1)\\ +\Omega_s[\omega_{\rm L}(\hat{\mathbf{z}}'\cdot\vec{\omega}_1)+i\omega(\hat{\mathbf{x}}'\cdot\vec{\omega}_1)]\\ -\omega_{\rm L}[\omega_{\rm L}(\hat{\mathbf{z}}'\cdot\vec{\omega}_1)+i\omega(\hat{\mathbf{x}}'\cdot\vec{\omega}_1)]\end{pmatrix}, \tag{75}$$

with $\Omega_s^2\equiv(\gamma^2/\chi)\,2g_{\rm D}\Delta_s^2$ given by

$$\Omega_s^2 = (\gamma^2/\chi)\,2g_{\rm D}\left[\Delta_{\rm A}^2-\tfrac{1}{2}\left(\bar\beta_4-\tfrac{1}{2}\bar\beta_5/\bar\beta_2\right)\Delta_z^2\right]. \tag{76}$$

The transverse resonance is at $\omega=\sqrt{\omega_{\rm L}^2+\Omega_s^2}$, with a maximum positive NMR frequency shift in the high-field limit $\omega_{\rm L}\gg\Omega_s$ given by

$$\Delta\omega\simeq\frac{1}{2}\,\Omega_s^2/\omega_{\rm L} = \frac{\gamma^2}{\chi\omega_{\rm L}}\,g_{\rm D}\left[\Delta_{\rm A}^2-\frac{1}{2}\left(\bar\beta_4-\frac{1}{2}\bar\beta_5/\bar\beta_2\right)\Delta_z^2\right]. \tag{77}$$

The predicted transverse shift is continuous at $T=T_{c_2}$, i.e., $\Delta\omega|_{T_{c_2}}=\frac{1}{2}\Omega_{\rm A}^2/2\omega_{\rm L}|_{T_{c_2}}$, but with a discontinuity in slope $\partial\Delta\omega/\partial T|_{T_{c_2}}$, governed by the polar distortion Δ_z, and GL coefficients $\bar\beta_{2,4,5}$. For $\bar\beta_4-\frac{1}{2}\bar\beta_5/\bar\beta_2>0$, we expect the polar distortion to lead to a reduction in the slope of the NMR shift below T_{c_2}.

However, as shown in Fig. 4, the data for the NMR shifts of ^{3}He in uniaxially stretched aerogel and reported by Pollanen *et al.*[19] show a more dramatic temperature dependence for the frequency shift below the second transition: a negative "jump" identified with T_{c_2}, followed by an increasing shift below T_{c_2}, but with a reduced slope compared to the ESP-1 phase above T_{c_2}. In addition, the NMR linewidth (shown in Fig. 3 of Ref. 19), which is sharp and virtually unchanged in the axially

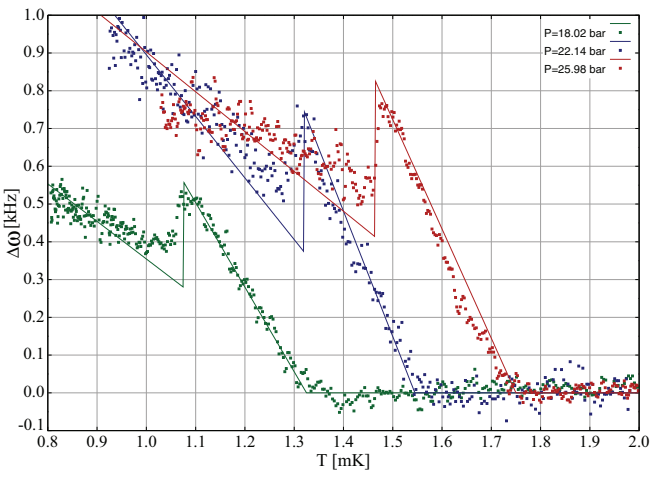

FIG. 4. (Color online) NMR frequency shifts for both ESP-1 and ESP-2 phases reproduced from Ref. 19 for pressures: 18 bar (green square), 22 bar (blue square), and 26 bar (red square). Theoretical curves for the same pressures are based on the predicted NMR shifts for the axially aligned ABM state (ESP-1) and the biaxial LIM phase (ESP-2) with a predicted negative jump of $\frac{1}{2}$ at T_{c_2}. The slopes are fits that are consistent with the theoretically predicted temperature dependencies for both ESP-1 and ESP-2 phases.

aligned ABM phase (ESP-1), increases rapidly below T_{c_2}. Both the jump in $\Delta\omega$ and the increased linewidth suggest that the ESP-2 phase exhibits some form of *orbital disorder* responsible for inhomogeneous broadening of the NMR spectrum and a reduction in the first moment (the shift). In the following, I consider orbital disorder, induced by random anisotropy, and its effects on the NMR spectrum for the biaxial phase.

First, consider the axially aligned ABM phase above T_{c_2} for which the chiral axis is aligned along the strain axis $\hat{\mathbf{l}} = \hat{\mathbf{z}}$. There is *no continuous orientational degeneracy* in the direction of the chiral axis. Thus, fluctuations in the local anisotropy axis of the aerogel contribute to the suppression of T_c and the magnitude of the order parameter, but long-range orientational order is preserved because there is a finite-energy cost to long-wavelength transverse fluctuations of the chiral axis.

A. Effect of random anisotropy on the biaxial phase

By contrast, the biaxial phase has a *continuous rotational degeneracy* corresponding to orientation of the chiral axis $\hat{\mathbf{l}}$, *on a cone* with angle ϑ fixed by the polar component of the order parameter [Eq. (62)] as shown Fig. 3. Fluctuations in the local anisotropy of the aerogel medium couple to the components of $\hat{\mathbf{l}}$ transverse to the strain axis and destroy long-range orientational order of the chiral axis:[20,30,31] more precisely, the *transverse* components of the chiral axis. In particular, the random-field averages of the biaxial triad are

$$\langle \hat{\mathbf{m}} \rangle = \sin\vartheta\, \hat{\mathbf{z}}, \quad \langle \hat{\mathbf{n}} \rangle = 0, \quad \langle \hat{\mathbf{l}} \rangle = \cos\vartheta\, \hat{\mathbf{z}}, \tag{78}$$

and the correlation function for the transverse components of the chiral axis $\delta\hat{\mathbf{l}} = \hat{\mathbf{l}} - \langle \hat{\mathbf{l}} \rangle$,

$$\langle \delta\hat{\mathbf{l}}_i(\mathbf{r}) \delta\hat{\mathbf{l}}_j(\mathbf{r}') \rangle \approx \tfrac{1}{2} \sin^2\vartheta\, (\delta_{ij} - \hat{\mathbf{z}}_i\hat{\mathbf{z}}_j)\, e^{-|\mathbf{r}-\mathbf{r}'|^2/2\xi_{\rm LIM}^2}, \tag{79}$$

exhibit short-range order up to a length scale $\xi_{\rm LIM}$ that depends on the microscopic model for the random anisotropy field and its coupling to the orbital order parameter (see Sec. VII). Nevertheless, different models for the random anisotropy field lead to orbital domain sizes that are typically smaller than the dipole coherence length.

In the limit $\xi_{\rm D} \gg \xi_{\rm LIM}$, the spin-orbit coupling of $\vec{\mathbf{d}}$ and $\hat{\mathbf{l}}$, and thus the NMR frequency shift, average to zero for a *globally isotropic* aerogel.[11,42] However, for the biaxial state in a *globally anisotropic* aerogel the random anisotropy field averaging leads to a spin-orbit coupling of $\vec{\mathbf{d}}$ and $\langle \hat{\mathbf{l}} \rangle \parallel \hat{\mathbf{z}}$:

$$\langle \Delta\Omega_{\rm D} \rangle = -2g_{\rm D} \left[\tfrac{1}{2}\Delta_{\rm A}^2 - \left(1 + \tfrac{1}{4}\bar{\beta}_4\right) \Delta_z^2 \right] (\vec{\mathbf{d}} \cdot \hat{\mathbf{z}})^2, \tag{80}$$

that is the same form as that for the axially aligned ABM phase (ESP-1), resulting in a transverse shift

$$\Delta\omega = \frac{\gamma^2}{\chi\omega_{\rm L}}\, g_{\rm D} \left[\frac{1}{2}\Delta_{\rm A}^2 - \left(1 + \frac{1}{4}\bar{\beta}_4\right) \Delta_z^2 \right], \tag{81}$$

which is *half* the transverse shift of the ESP-1 phase for $T \to T_{c_2}$ from below. Thus, the orbitally disordered biaxial phase exhibits a "negative jump" of the NMR shift to half that of the ESP-1 NMR shift and a reduction in the slope of the shift for $T < T_{c_2}$. This result is in good agreement with the observed temperature dependence of the NMR shifts reported by Pollanen *et al.*[19] as shown in Fig. 4. The theoretical slopes are fit to the experimental results, and are in agreement with theoretical expectations based on Eqs. (18) and (81).

The predicted jump of $\frac{1}{2}$ is the maximum reduction in the shift resulting from the averaging the triad of orbital vectors over a cone with fixed polar angle ϑ. The magnitude of the jump is reduced if the transverse components $\delta\hat{\mathbf{l}}$ are not uniformly distributed on the cone shown in Fig. 3. Furthermore, since $\sin\vartheta \sim \Delta_z(T) \to 0$ as $T \to T_{c_2}$ we have $\hat{\mathbf{l}} \to \hat{\mathbf{z}}$. Thus, averaging on the collapsing cone becomes irrelevant sufficiently close to T_{c_2}, and we must recover the full EPS-1 NMR shift continuously over a narrow temperature "width" of order $\delta T_{c_2} \simeq T_{c_2}(\xi_{\rm LIM}/\xi_D)^2 \ll T_{c_2}$ as the cone angle closes towards the axially aligned ABM phase (see Sec. IX). Such a crossover very close to T_{c_2} is visible in Fig. 4 with observed "widths" of order $\delta T_{c_2} \approx 0.1$ mK, providing an estimate for the orbital domain size of $\xi_{\rm LIM} \approx \frac{1}{3}\xi_{\rm D} \approx 5\ \mu$m at 18 bar. Orbital domains of size $\xi_{\rm LIM} \lesssim \xi_{\rm D}$ also provide a plausible explanation for the onset of increased NMR linewidth observed just below T_{c_2}. But, are such large domains of the orbital order parameter plausible?

Volovik addressed the issue of orbital disorder in superfluid ^{3}He induced by random anisotropy[20,42] and derived a formula for the domain size based on arguments similar to those of Larkin[30] and Imry and Ma.[31] Volovik's result for the LIM correlation length[20]

$$\xi_{\rm LIM}^{\rm Volovik} = \xi_a(\xi_0/d)^2 \tag{82}$$

is based on (i) anisotropy derived from randomly oriented cylinders of mean spacing $\xi_a \approx 20$ nm and diameter $d \approx 3$ nm, representing the aerogel, and (ii) the orientational energy for a single cylindrical impurity in bulk ^{3}He-A calculated by Rainer and Vuorio, $E_a \approx T_c\, k_f^2\, \xi_a\, d$.[21] This gives an orbital correlation length $\xi_{\rm LIM}^{\rm Volovik} \lesssim 1\ \mu$m, weakly pressure dependent and an order of magnitude or more smaller than the dipole coherence length $\xi_{\rm D}$ (black curves in Fig. 6). The ratio $\xi_{\rm LIM}^{\rm Volovik}/\xi_{\rm D}$ decreases dramatically at lower pressures. Implicit in this calculation is the assumption that the single impurity result of Ref. 21 extends to a distribution cylindrical impurities with typical spacing ξ_a that is less than or the same order as the pair correlation length ξ_0. Indeed, the fractal structure of the aerogel on length scales *shorter* than ξ_a may be responsible for weaker local anisotropy and thus a larger orbital domain size than the estimate from Eq. (82).[22]

VII. ANISOTROPIC SCATTERING MODEL

Silica aerogels grow by gelation of silica clusters. The resulting structure factors measured by SAXS on high-porosity silica aerogels are in good agreement with numerical simulations based on diffusion-limited-cluster aggregation (DLCA).[25,26] A DLCA simulation of 98% aerogel is presented in Fig. 5 showing structures that are locally anisotropic, as well as statistically self-similar over several decades in length scales. The aerogel correlation length ξ_a is characteristic of the largest "void" dimension, while the microscopic scale is indicated by the "strand" width $d \ll \xi_a$ in Fig. 5. Note that local anisotropy results from clusters and strands with multiple length scales.

In the following, I formulate a model of the random field in aerogels, including random anisotropy, in terms of the distribution of ballistic paths for quasiparticles propagating

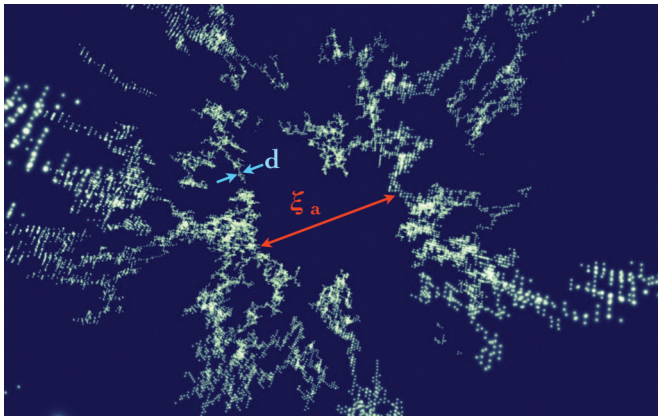

FIG. 5. (Color online) Local anisotropy of silica clusters and strands based on a DLCA simulation for the growth of a 98% porous aerogel. Statistical self-similarity is observable over three decades of length scales. The aerogel correlation length is of order $\xi_a \simeq 30$ nm, while the strand size is of order $d \simeq 2$ nm.

through the open regions of aerogel. Elastic scattering by the fractal structure limits ballistic propagation. The local cross section, or scattering rate, is then the measure of random anisotropy. Such a description was discussed by Thuneberg *et al.*[11,12] as a course-grained model of random anisotropy compared to the atomic scale d of a silica strand. In the following, I expand on this model.

The scattering of quasiparticles by the aerogel is formulated in terms of the amplitude $u(\mathbf{p},\mathbf{p}')$ for quasiparticle transitions from $\mathbf{p} \to \mathbf{p}'$ for a random distribution of scattering centers ("strands" or "clusters") with average density n_s. At low temperatures $T \ll E_f$, the elastic scattering rate is

$$\frac{1}{\tau_{\mathbf{p},\mathbf{p}'}} \equiv w(\mathbf{p},\mathbf{p}') = \pi\, n_s\, N_f\, |u(\mathbf{p},\mathbf{p}')|^2, \tag{83}$$

where N_f is the quasiparticle density of states at the Fermi energy. If the scattering medium is locally isotropic, the scattering rate may be expanded in Legendre functions, e.g., $w(\mathbf{p},\mathbf{p}') = w_0 + w_1\, \hat{\mathbf{p}}\cdot\hat{\mathbf{p}}' + \cdots$, where I include s- and p-wave scattering. However, the scattering centers are anisotropic. On mesoscopic length scales $d \ll \delta r < \xi_a$ the anisotropy is locally well defined, and the scattering rate will depend on the directions of the incident and scattered quasiparticle momenta *relative* to a set of anisotropy axes defining a local region of scattering centers. This is illustrated by considering a medium of randomly distributed but identical cylindrical "strands." The scattering medium is then locally uniaxial and the scattering rate is determined by the local orientation of the anisotropy axis of the strand, defined by $\hat{\mathbf{s}}$.[43] For this "strand model" the scattering rate in the s-p approximation,

$$\frac{1}{\tau_{\mathbf{p},\mathbf{p}'}} = w_0 + \hat{\mathbf{p}}_i\, w_{ij}\, \hat{\mathbf{p}}'_j \tag{84}$$

is parametrized by an isotropic scattering rate w_0 and a uniaxial tensor

$$w_{ij} = w_\perp\,(\delta_{ij} - \hat{\mathbf{s}}_i\hat{\mathbf{s}}_j) + w_\parallel\,\hat{\mathbf{s}}_i\hat{\mathbf{s}}_j \tag{85}$$

with p-wave scattering rates $w_{||}$ and $w_\perp$ for scattering preferentially along the symmetry axis and perpendicular to the symmetry axis, respectively. The random anisotropy field for the strand model is then encoded in the distribution of of the local anisotropy axis $\hat{\mathbf{s}}(\mathbf{r})$.[44] For a *globally isotropic medium,* the anisotropic scatters remain oriented over a finite correlation length ξ_s defined by the decay of the orientational correlations

$$\langle \hat{\mathbf{s}}(\mathbf{r})\cdot\hat{\mathbf{s}}(0)\rangle \sim e^{-r^2/2\xi_s^2}, \tag{86}$$

where the configurational average can be defined in terms of a joint probability distribution for the orientation of all impurities. A reasonable estimate for this correlation length based on the DLCA simulations is the aerogel correlation length $\xi_a \approx 30$–50 nm.

The relative scale of the orientational correlations to that of the pair correlation length ξ_0 is an important parameter. For $\xi_s \gg \xi_0$, scattering by the aerogel structure leads to anisotropic pair-breaking effects on the orbital states of p-wave Cooper pairs, and a splitting of the superfluid transition for Cooper pairs with orbital motion parallel and perpendicular to the anisotropy direction $\hat{\mathbf{s}}$, i.e., $T_{c\perp} \neq T_{c||}$, as discussed in Sec. VIII. In the opposite limit $d \ll \xi_s \ll \xi_0$, the aerogel medium is on average isotropic on length scales larger than ξ_s. As a result, the orbital p-wave components are unstable at the same transition temperature, i.e., there is a single T_c. However, the transition and the relative stability of the possible phases will generally be modified by the short-range anisotropic scattering. In both limits, *random anisotropy* leads to formation of orbital domains (LIM effect) on length scales that are typically longer than either the aerogel or pair correlation lengths ξ_s and ξ_0. For ^{3}He in low-density silica aerogels, $\xi_s \lesssim \xi_0$, with the two correlation lengths being comparable at high pressures $p \gtrsim 15$ bar. And as I discuss in Sec. IX, the LIM effect is controlled not only by competition between orbital order and orientational energetics at the scale of ξ_s, but also by random anisotropy in ballistic transport. The latter determines the random field for Cooper pairs when $\xi_s \lesssim \xi_0$.

VIII. LONG-RANGE ORDER OF ANISOTROPIC IMPURITIES

Silica aerogels with exceptional homogeneity and global anisotropy have been fabricated,[45] and global anisotropy can be induced by uniaxial compression of an isotropic aerogel. Global anisotropy in these aerogels corresponds to long-range order of the locally anisotropic scattering medium

$$\langle \hat{\mathbf{s}}(\mathbf{r})\cdot\hat{\mathbf{s}}(0)\rangle \xrightarrow[r\gg\xi_s]{} s^2, \tag{87}$$

where $0 < s^2 < 1$ measures the degree of long-range orientational order along the uniaxial anisotropy, or strain, axis $\hat{\mathbf{z}}$. Random fluctuations of the anisotropy direction remain, but are uncorrelated over distances larger than ξ_s.

Long-range order of the strands is directly observable in transport properties of normal ^{3}He in a globally anisotropic aerogel. At temperatures below the crossover scale $T^\star \approx$ 20–30 mK, the transport of entropy and magnetization is determined by elastic scattering of quasiparticles from the aerogel structure. For example, the thermal conductivity becomes anisotropic below $T^\star$ (Ref. 46):

$$\kappa_{ij} = \frac{2\pi^2}{9}\, N_f\,(v_f T)\,\bar{\ell}_{ij}, \tag{88}$$

where $\bar{\ell}_{ij}$ is the transport *mfp* tensor obtained from the Boltzmann-Landau transport equation with the collision integral determined by the elastic scattering rate in Eq. (84):

$$\bar{\ell}_{ij} = \bar{\ell}_\perp(\delta_{ij} - \hat{\mathbf{z}}_i\hat{\mathbf{z}}_j) + \bar{\ell}_\parallel\,\hat{\mathbf{z}}_i\hat{\mathbf{z}}_j, \tag{89}$$

where $\bar{\ell}_\perp = v_f\tau_\perp$ ($\bar{\ell}_\parallel = v_f\tau_\parallel$) is the transport *mfp* for heat transport perpendicular (parallel) to the anisotropy axis. Hydrodynamic transport averages over length scales long compared to ξ_s, thus long-range orientational order determines the anisotropy of the transport coefficients with

$$\frac{1}{\tau_\perp} = \frac{1}{\bar{\tau}} + \frac{1}{3}\Delta, \quad \frac{1}{\tau_\parallel} = \frac{1}{\bar{\tau}} - \frac{2}{3}\Delta, \tag{90}$$

$$\frac{1}{\bar{\tau}} = w_0 - \frac{1}{3}\left(\frac{2}{3}\,w_\perp + \frac{1}{3}\,w_\parallel\right), \tag{91}$$

$$\Delta = -\frac{1}{3}\,s^2\,(w_\perp - w_\parallel). \tag{92}$$

Note that the anisotropy in the scattering rates Δ scales as the product of the long-range orientational order of the anisotropic "impurities" $\sim s^2$, and the (local) anisotropy of the p-wave scattering rates $\sim(w_\perp - w_\parallel)$. In the absence of orientational fluctuations ($s = 1$) we obtain the maximal anisotropy in the scattering rates: $1/\tau_\perp = 1/\tau_0 - \frac{1}{3}w_\perp$, $1/\tau_\parallel = 1/\tau_0 - \frac{1}{3}w_\parallel$, and $(1/\tau_\perp - 1/\tau_\parallel) = -\frac{1}{3}(w_\perp - w_\parallel)$. In the absence of long-range orientational order ($s = 0$), $\Delta = 0$, and the local anisotropy gives an average isotropic scattering rate and *mfp*, $\bar{\ell} = v_f\bar{\tau}$.

The *mfp* anisotropy obtained from Eqs. (90)–(92) determines the splitting of the superfluid transition when the aerogel correlation length ξ_s is smaller than the size of Cooper pairs. This is the *homogeneous scattering limit* in which quasiparticle scattering from the aerogel is the dominant pair-breaking effect.[11,12] For a globally anisotropic scattering medium, the pair-breaking effect is also symmetry breaking, lifting the degeneracy of the 3D p-wave orbital states and splitting the transition for pairing into 2D orbital states ($\hat{\mathbf{p}}_x$,$\hat{\mathbf{p}}_y$), and pairing into the 1D polar state $\hat{\mathbf{p}}_z$.[11,13] The corresponding second-order GL coefficients that enter Eq. (3) for 2D and 1D orbital states are[11]

$$\bar{\alpha}_{\perp,\parallel} = \tfrac{1}{3}\,N_f\,[\ln(T/T_c) - \mathscr{S}_1(x_{\perp,\parallel}\,T_c/T)], \tag{93}$$

where $x_{\perp,\parallel} = \xi_0/\bar{\ell}_{\perp,\parallel}$ are the anisotropic pair-breaking parameters, and $\mathscr{S}_1(z)$ is the digamma function

$$\mathscr{S}_1(z) = \sum_{n=0}^{\infty}\left[\frac{1}{n+\frac{1}{2}+\frac{1}{2}z} - \frac{1}{n+\frac{1}{2}}\right]. \tag{94}$$

The instability temperatures for superfluid ^{3}He in a globally anisotropic medium are given by $\alpha(T_{c_{\perp,\parallel}}) = 0$, and are the solutions to the Abrikosov-Gorkov equation[47]

$$\ln(T_c/T_{c_{\perp,\parallel}}) = \mathscr{S}_1(x_{\perp,\parallel}\,T_c/T_{c_{\perp,\parallel}}). \tag{95}$$

In the linear pair-breaking regime, we obtain

$$T_{c_{\perp,\parallel}} \simeq T_c\left(1 - \frac{\pi^2}{4}\,\frac{\xi_0}{\bar{\ell}_{\perp,\parallel}}\right), \tag{96}$$

where $\xi_0 = \hbar v_f/2\pi\,k_B\,T_{c_0}$ (T_{c_0}) is the pair correlation length (transition temperature) for pure ^{3}He. Thus, for $\bar{\ell}_\perp > \bar{\ell}_\parallel$ the first instability will be to a 2D orbital state with the 2D orbital order parameter $\bar{a} \neq 0$, while for $\bar{\ell}_\perp < \bar{\ell}_\parallel$ the first instability will be into the 1D polar state with $b \neq 0$. The orbital representation that is realized at the first instability for a "stretched" or mechanically compressed aerogel depends on the microscopic mechanism(s) for the development of global anisotropy in the ballistic path length distribution for quasiparticles in anisotropic aerogel. The splitting of the transition

$$\frac{T_{c_\perp} - T_{c_\parallel}}{T_c} \simeq -\frac{\pi^2}{4}\,\xi_0\left(\frac{1}{\bar{\ell}_\perp} - \frac{1}{\bar{\ell}_\parallel}\right) \tag{97}$$

is proportional to the difference in the mean scattering rates, which scales as $(1/\tau_\perp - 1/\tau_\parallel) = -\frac{1}{3}s^2\,(w_\perp - w_\parallel)$. Thus, the splitting of the transition may be significantly smaller than the suppression of the superfluid transition from that of pure ^{3}He, which depends on the total scattering rate [Eq. (90)]. This provides a natural explanation for the relatively large-T_c suppression and relatively small-T_c splitting shown Fig. 1, which at 18 bar is a suppression of $T_c - T_{c_\perp} \simeq 0.84$ mK, and a splitting $T_{c_\perp} - T_{c_\parallel}$ less than 0.28 mK. This leads us to a prediction for ^{3}He in the stretched aerogel.[19] If long-range order of anisotropic scattering centers is the mechanism for stabilizing the 2D chiral ABM state in stretched aerogel, then measurements of heat transport in normal ^{3}He should show anisotropy with $\kappa_\perp/\kappa_\parallel = \bar{\ell}_\perp/\bar{\ell}_\parallel > 1$. Furthermore, if the ESP-2 state is the signature of the biaxial phase associated with the onset of the polar distortion and a nonvanishing $0 < T_{c_\parallel} < T_{c_\perp}$, then the ratio for $\kappa_\perp/\kappa_\parallel$ can be predicted from the splitting of the transitions and the β parameters obtained from NMR and thermodynamic measurements on these phases.

Finally, note that for sufficiently strong anisotropy, the second instability may be suppressed to zero, or to temperatures well outside the GL limit. This limit is likely relevant to superfluid ^{3}He reported in the newly discovered "nematic" aerogels with *mfp*'s of $\bar{\ell}_\parallel = 850$ nm and $\bar{\ell}_\perp = 450$ nm based on measurements of spin diffusion in the normal state.[37] The anisotropy ratio $\bar{\ell}_\parallel/\bar{\ell}_\perp \approx 2$ favors a transition from the normal state into the *1D polar phase* based on this theory of homogeneous anisotropic pair breaking. Nematic aerogels appear to be inhomogeneous on the scale of ξ_0, so this theory may account for a transition to the polar state near $T_{c_\parallel}$, where $\xi(T) \gg \xi_a$, but is likely outside the regime of validity to describe the low-temperature phases.

IX. RANDOM ANISOTROPY

The biaxial phase described in Secs. V and VI that onsets below T_{c_2} has a continuous degeneracy corresponding to rotations of the orbital triad $\{\hat{\mathbf{m}},\hat{\mathbf{n}},\hat{\mathbf{l}}\}$ about the uniaxial "stretch" axis $\hat{\mathbf{z}}$. The latter is interpreted here as a manifestation of long-range orientational order of the scattering centers with $\langle\hat{\mathbf{s}}\rangle = s\hat{\mathbf{z}}$. Fluctuations in the local anisotropy axis $\mathbf{s}'(\mathbf{r}) = \hat{\mathbf{s}} - s\hat{\mathbf{z}}$ couple to the orbital order parameter and partially destroy the long-range orientational order of the biaxial phase.

The *random* anisotropy energy is defined by the fluctuations in the pair-breaking effect given by

$$\Delta\Omega_{\rm an} = \int_{\rm V} d^3\,\delta\,\alpha_{ij}(\mathbf{r})\,\mathscr{A}_i\,\mathscr{A}_j^*, \tag{98}$$

where the leading-order term of $\delta\alpha_{ij}(\mathbf{r}) = \alpha_{ij}(\mathbf{r}) - \bar{\alpha}_{ij}$ for weak global anisotropy ($s^2 \ll 1$) is

$$\delta\alpha_{ij} = -\tfrac{1}{2}\,\delta\alpha\,\left(\mathbf{s}'_i(\mathbf{r})\,\mathbf{s}'_j(\mathbf{r}) - \tfrac{1}{3}\right), \tag{99}$$

$$\delta\alpha = (\pi^2/4)\,N_f\,\xi_0\,(1/\ell_\parallel - 1/\ell_\perp)\,[\mathscr{S}_2(\bar{x})/\mathscr{S}_2(0)]\,. \tag{100}$$

Note that the random anisotropy is enhanced compared to the global anisotropy by the factor $1/s^2$, i.e., $(1/\ell_\parallel - 1/\ell_\perp) = \frac{1}{3}(w_\parallel - w_\perp) = (1/\bar{\ell}_\parallel - 1/\bar{\ell}_\perp)/s^2$. Also, I include the mean-field pair-breaking effects with $\bar{x} = \hbar/2\pi T_c\bar{\tau} = \xi_0/\bar{\ell}$, the suppression of T_c by impurity scattering and the functions

$$\mathscr{S}_p(x) \equiv \sum_{n\geqslant 0}\left(n + \frac{1}{2} + \frac{1}{2}x\right)^{-p}, \quad p > 1 \tag{101}$$

that renormalize the GL coefficients.[11,48]

The random anisotropy energy obtained from Eqs. (98)–(100) and (63), the completeness relation $\delta_{ij} = \hat{\mathbf{m}}_i\hat{\mathbf{m}}_j + \hat{\mathbf{n}}_i\hat{\mathbf{n}}_j + \hat{\mathbf{l}}_i\hat{\mathbf{l}}_j$ and $\Delta_z^2 \ll \Delta_{s,d}^2$ for $T \lesssim T_{c_2}$ becomes

$$\Delta\Omega_{\rm an} = -\frac{1}{2}\,\delta\alpha\,\Delta_s^2\int_{\rm V} d^3r\,\left[[\mathbf{s}'(\mathbf{r})\cdot\hat{\mathbf{l}}(\mathbf{r})]^2 - \frac{1}{3}\right], \tag{102}$$

where $\hat{\mathbf{l}}(\mathbf{r})$ is the local chiral axis in the biaxial phase. The mean field orientation for $\hat{\mathbf{l}}$ is fixed on the cone shown in Fig. 3. The transverse orbital order parameter $\delta\hat{\mathbf{l}} = \hat{\mathbf{l}} - \bar{l}_z\hat{\mathbf{z}}$ is degenerate and can point in any direction in the base of the cone.

The fluctuations in the anisotropy of the scattering medium are correlated on the scale of ξ_s. Thus, the minimum of the random anisotropy energy is achieved by having the chiral axis $\hat{\mathbf{l}}(\mathbf{r})$ "track" the transverse fluctuations in anisotropy, i.e., $\delta\hat{\mathbf{l}}(\mathbf{r}) \parallel \mathbf{s}'_\perp(\mathbf{r})$. However, tracking the anisotropy on the scale of ξ_s costs gradient energy of order

$$\Delta\Omega_{\rm grad} = \kappa\,\Delta_s^2\int_{\rm V} d^3r\,|\nabla_i\,\hat{\mathbf{l}}_j|^2 \approx V\,\left(\kappa\,\sin^2\vartheta\,\Delta_s^2\,\xi_s^{-2}\right), \tag{103}$$

with $\kappa = \frac{4}{15}[7\zeta(3)/8]N_f\xi_0^2\,[\mathscr{S}_3(\bar{x})/\mathscr{S}(0)]$,[11] which gives a gradient energy that is larger than the condensation energy for $\xi_s < \xi_0$ and $T < T_{c_2}$. The balance between the local anisotropy energy and the gradient energy leads to the *partial* destruction of long-range orbital order for the biaxial phase in which $\langle\hat{\mathbf{l}}\rangle = \bar{l}_z\,\hat{\mathbf{z}}$, but long-range order of the transverse orbital order parameter $\delta\hat{\mathbf{l}}$ is destroyed.

The competition between the random anisotropy energy [Eq. (102)] and the gradient energy leads to short-range transverse orbital order over length scales $\xi_{\rm LIM} \gg \xi_s$, i.e., the Larkin-Imry-Ma (LIM) domain size. The argument here is similar to that discussed by Volovik,[20] but with different energy and length scales ultimately determining $\xi_{\rm LIM}$. In the presence of the random anisotropy field, the biaxial phase can avoid large gradient energies by allowing $\delta\hat{\mathbf{l}}$ to remain nearly uniform over length scales of order $\xi_{\rm LIM} \gg \xi_0 > \xi_s$. Thus, $\xi_{\rm LIM}$ is the domain size characterizing the short-range transverse orbital order. The cost in gradient energy to bend the order parameter over the same length scale is significantly reduced compared to Eq. (103), but so too is the gain in the random anisotropy energy. The latter is reduced by the fraction of anisotropy domains with $\mathbf{s}'$ favorably aligned with the transverse order parameter $\delta\hat{\mathbf{l}}$ within an orbital domain. Within an orbital domain of volume $V_{\rm LIM} = \xi_{\rm LIM}^3$, the mean number of domains of the anisotropy axis $\mathbf{s}'_\perp$ is $N_s = (\xi_{\rm LIM}/\xi_s)^3 \gg 1$. The fraction of anisotropy domains that can favorably be aligned is the fluctuation ratio $f_{\rm an} = \Delta N_s^{\rm rms}/N_s = 1/\sqrt{N_s} \approx (\xi_s/\xi_{\rm LIM})^{3/2}$. With this estimate, the optimal domain size is determined by minimizing the fluctuation of the anisotropy energy together with the gradient energy[20,31]

$$\Delta\Omega_{\rm fluc} = V\,\sin^2\vartheta\,\Delta_s^2\left(-\tfrac{1}{3}\,\delta\alpha\,(\xi_s/\xi_{\rm LIM})^{3/2} + \kappa\,\xi_{\rm LIM}^{-2}\right), \tag{104}$$

which gives the LIM domain size

$$\xi_{\rm LIM} = \left(\frac{4\kappa}{\delta\alpha}\right)^2\xi_s^{-3} = C_{\rm L}\,\frac{\xi_0^2\xi_s^{-3}}{[1/\ell_\parallel - 1/\ell_\perp]^2}, \tag{105}$$

$$C_{\rm L}(\bar{x}) = \left(\frac{4}{15}\right)^2\left(\frac{4}{\pi}\right)^4\left(\frac{7\zeta(3)}{8}\right)^2\left[\frac{\mathscr{S}_3(\bar{x})/\mathscr{S}_3(0)}{\mathscr{S}_2(\bar{x})/\mathscr{S}_2(0)}\right]^2, \tag{106}$$

where $C_{\rm L}(\bar{x})$ includes the renormalization of κ and $\delta\alpha$ due to the breaking of Cooper pairs by quasiparticle scattering, parametrized by $\bar{x} = \xi_0/\bar{\ell}$. In the limit $\bar{x} \to 0$, $C_{\rm L}(0) \simeq 0.21$.

Figure 6 shows the pressure dependence of the LIM domain size calculated from Eqs. (105) and (106) for an anisotropic aerogel defined by an average *mfp*, $\bar{\ell} = 120$ nm and the random field anisotropy of the aerogel expressed in terms of the anisotropy in the *mfp*'s, $\delta\ell/\ell = 2\%$–20%.[49] The mean-field effect of impurity scattering is included via the impurity scattering renormalization of the transition temperature T_c/T_{c_0}, the gradient coefficient $\kappa \sim \mathscr{S}_3(\bar{x})/\mathscr{S}_3(0)$, and the random anisotropy coefficient $\delta\alpha \sim \mathscr{S}_2(\bar{x})/\mathscr{S}_2(0)$. I also show the pressure dependence of the dipole coherence length. The LIM effect on the NMR frequency shift depends on the relative size of the orbital domains to the dipole coherence length $\xi_{\rm D} = \sqrt{\kappa/g_{\rm D}}$ since $\vec{\mathbf{d}}$ can adjust to the local orbital order only on length scales larger than $\xi_{\rm D}$.[20] The dipole coupling constant is unrenormalized by impurity scattering,[11] and is fixed at each pressure by the measured bulk A-phase NMR shift.[50] The resulting curves for $\xi_{\rm D}$ for bulk ^{3}He (dotted red curve) and ^{3}He-aerogel for $\bar{\ell} = 120$ nm (solid red curve) are shown for comparison with $\xi_{\rm LIM}$. Note that the critical pressure for this aerogel, below which superfluidity is suppressed, is $p_c \approx 8$ bar. The main result is that the orbital domain size is typically $\xi_{\rm LIM} \lesssim \xi_{\rm D}$ over the full pressure range, and may be larger than $\xi_{\rm D}$ for relatively weak random anisotropy $\Delta\ell/\ell \lesssim 5\%$.

Also shown in Fig. 6 is the LIM domain size obtained from the rigid cylinder model of random anisotropy proposed by Volovik; the solid black curve includes the impurity renormalization of the gradient coefficient [not shown in Eq. (82)]. The suppression of $\xi_{\rm LIM}^{\rm Volovik} \to 0$ for $p \to p_c$ is likely an artifact of the single-impurity model for the random anisotropy energy from Rainer and Vuorio.[21] Away from p_c $\xi_{\rm LIM}^{\rm Volovik} < 1\ \mu$m over the full pressure range, implying that orbital order is destroyed by a relatively strong random anisotropy field over length scales much smaller than $\xi_{\rm D}$ at all pressures ($\xi_{\rm LIM}^{\rm Volovik} \approx 0.77\ \mu$m compared to $\xi_{\rm D} \approx 16.1\ \mu$m at 18 bar). The conclusion here is that the random anisotropy field that is relevant to the destruction of orbital order, and

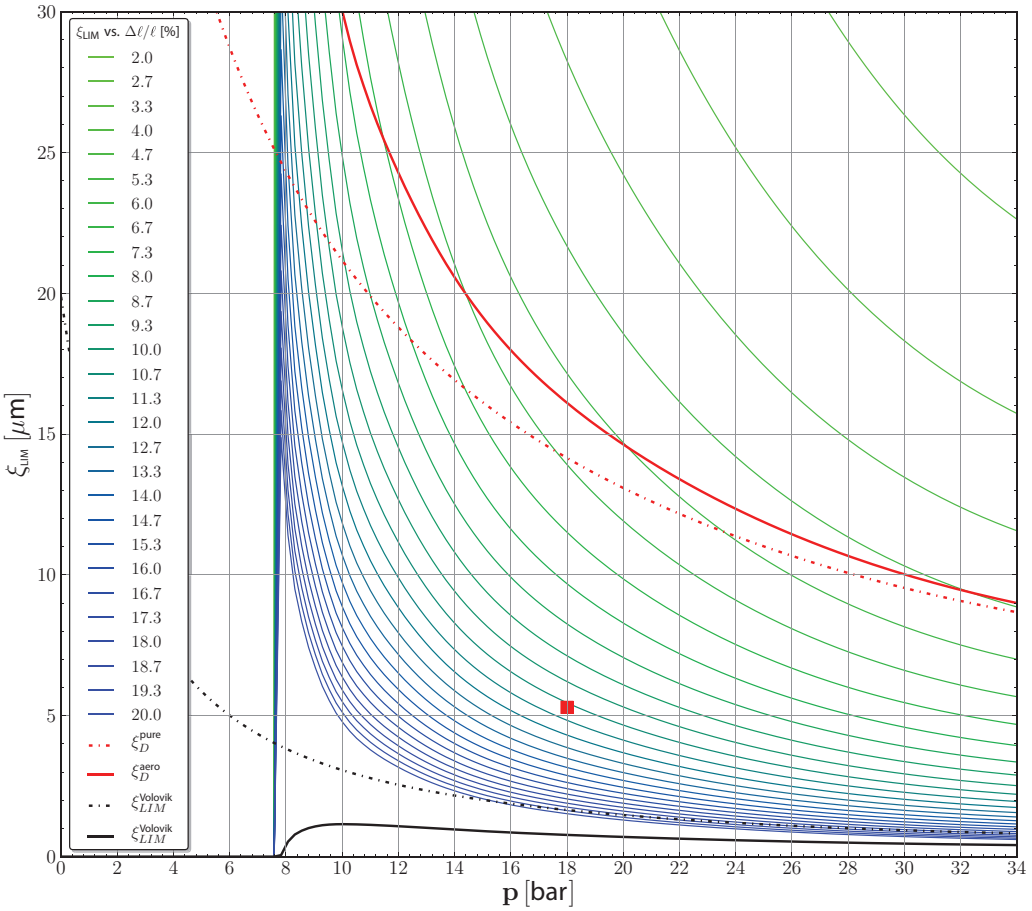

FIG. 6. (Color online) Larkin-Imry-Ma domain size for the biaxial orbital order parameter as a function of pressure for aerogel with average *mfp* $\ell = 120$ nm, strand correlation length $\xi_s = 20$ nm, and anisotropy ranging from $\Delta\ell/\ell = 2\%$–20% (blue-green curves). Volovik's result for the LIM length (black dashed curve), while the (black solid curve) includes the renormalization of the parameters defining the LIM length due to pair breaking for an aerogel with $T_c(p)$ determined by $\bar{x} = \xi_0/\bar{\ell}$. The dipole coherence length ξ_D is shown as the (solid red curve) for the same *mfp*, and for pure ^{3}He as the (dashed red curve). The point (red square) at 18 bar is $\xi_{LIM} \approx 5.3$ μm determined from the width of the negative jump in the NMR shift shown in Fig. 4.

the LIM domain size, can be much weaker, originating from mesoscale structures that are much larger than atomic scale $d \ll \delta r \ll \xi_a$, and are responsible for local anisotropy in the quasiparticle scattering rate.

In the weak anisotropy limit, the LIM averaging of the dipole energy breaks down and we expect a distribution of NMR shifts resulting from the distribution of spatial variations of the dipole energy on the scale $\xi_{LIM} \sim \xi_D$. The NMR spectra for the stretched aerogel, particularly the rapid reduction in the shift below T_{c_2} and the broadening of the line, suggests that $\xi_{LIM} \lesssim \xi_D$. In this case, the orienting effect on the orbital order parameter of the biaxial phase by the dipole energy can be treated perturbatively. For $T \ll T_{c_2}$, the polar distortion is established, $\hat{\mathbf{l}}$ is oriented off the anisotropy axis, and the transverse orbital order parameter $\delta\hat{\mathbf{l}} = \sin\vartheta(\cos\varphi\hat{\mathbf{x}} + \sin\varphi\hat{\mathbf{y}})$ is degenerate on the cone in Fig. 3. Optimizing the random anisotropy energy and the gradient energy for the transverse orbital order leads to the optimal orbital domain size given by Eq. (105). These two energies are of the same order with an overall magnitude that scales as $\Delta_s^2 \sin^2\vartheta \sim \Delta_z^2 \sim (1 - T/T_{c_2})$. Thus, sufficiently close to T_{c_2}, the dipole energy will become comparable to the optimized random field domain-alignment energy. The dipole energy can now compete to align the transverse orbital order parameter and recover dipole energy that was "lost" by averaging $\delta\hat{\mathbf{l}}$ on the cone. At high fields $\omega_L \gg \Omega_A$, $\vec{\mathbf{d}}$ is fixed perpendicular to the field, e.g., $\vec{\mathbf{d}} \perp \hat{\mathbf{y}}$ in Fig. 3. The competition between the fluctuation contribution to the dipole energy and random field domain-alignment energies converts the jump in $\Delta\omega$ at T_{c_2} into a crossover with a transition width δT_{c_2}, given by the temperature at which the "missing" dipole energy becomes equal to the stiffness of the biaxial LIM state

$$\frac{1}{2} g_D \Delta_A^2 = \kappa \, \sin^2\vartheta \, \Delta_s^2 \, \xi_{LIM}^{-2} \simeq 2\kappa \, \Delta_z \big(T_{c_2} + \delta T_{c_2}\big)^2 \, \xi_{LIM}^{-2} \tag{107}$$

$$\rightsquigarrow \delta T_{c_2} = T_{c_2} \times \frac{1}{4} \left(\frac{\Delta_A}{\bar{\Delta}_z}\right)^2 \left(\frac{\xi_{LIM}}{\xi_D}\right)^2 . \tag{108}$$

For the $\bar{\Delta}_z/\Delta_A \approx 2$ at T_{c_2}, we obtain the estimate of $\xi_{LIM} \approx 5$ μm from the observed transition width of $\delta T_{c_2}/T_{c_2} \approx 0.1$ at 18 bar, which based on random field anisotropy in the scattering rate corresponds to $\Delta\ell/\ell \simeq 11\%$. For comparison,

the authors of Ref. 19 characterize the "stretched" aerogel in their NMR experiments by uniaxial strain $\varepsilon_{zz} \simeq 14\%$.

X. SUMMARY AND CONCLUSIONS

The discovery of equal-spin-pairing (ESP) phases of superfluid ^{3}He in highly porous *anisotropic* silica aerogels provides us with a unique condensed matter system for investigation of remarkable phases that may be realized in systems with broken continuous symmetries and competing effects from disorder. A Ginzburg-Landau (GL) theory for orbital p-wave phases in a medium with both global and random anisotropy was developed. Global anisotropy gives rise to multiple ordered phases that are characterized as 2D (chiral or in-plane polar), 1D axial aligned polar states, and a "mixed"-symmetry phase that exhibit both biaxial and chiral order, depending on the nature of the *global* anisotropy, e.g., stretched versus compressed anisotropy. The 2D chiral phase is an ABM state with the chiral axis aligned *along* the anisotropy axis in the case of "stretched" aerogels, i.e., $\hat{\mathbf{l}} = \pm\hat{\mathbf{z}}$. The NMR signatures of the 2D chiral phase with $\hat{\mathbf{l}} \parallel \pm\hat{\mathbf{z}}$ are in quantitative agreement with the ESP-1 phase of ^{3}He in "stretched aerogel" reported in Ref. 19, including a large transverse shift, the tipping angle dependence, *and* a narrow linewidth. The ESP-1 phase cannot be identified with a chiral phase with $\hat{\mathbf{l}} \perp \hat{\mathbf{z}}$. Not only is this phase excluded by symmetry for a uniform uniaxial medium, if it were present as a second, low-temperature phase it would exhibit a reduced NMR shift and a broadened NMR line due to the LIM effect. Additional support for this identification is provided by recent NMR measurements[51] on ^{3}He infused into the same "stretched aerogel" as in Ref. 19, but with the static NMR field along the strain axis and the rf field perpendicular to the strain axis. In this orientation, the NMR shift that onsets at the same T_{c_1} as in Ref. 19 is *negative* as is expected for an ESP-1 phase with $\hat{\mathbf{l}} \parallel \pm\hat{\mathbf{z}}$. In contrast, a chiral phase with $\hat{\mathbf{l}} \perp \hat{\mathbf{z}}$ should exhibit a positive shift for both field configurations. Furthermore, the results of Li *et al*. exclude the normal to 1D polar phase scenario since the polar phase, were it the present, would show a large positive shift onsetting at a temperature *above* T_{c_1} as measured by Pollanen *et al*. No such transition is observed. Thus, the analysis presented here combined with the experiments of Refs. 19 and 51 show that the ESP-1 phase is a chiral ABM state with $\hat{\mathbf{l}} \pm \hat{\mathbf{z}}$.

The biaxial phase spontaneously breaks the rotational symmetry about the global anisotropy axis, and is identified with the ESP-2 phase of ^{3}He in stretched aerogel. This identification depends upon the interplay between the continuous degeneracy of the biaxial phase, associated with broken $U(1)_{L_z-N}$ rotational symmetry, and *random* anisotropy associated with the structure of the aerogel. Comparison of the NMR spectrum for the ESP-2 phase with theoretical predictions for the NMR frequency shifts provides strong evidence for identifying the ESP-2 as the biaxial state, partially *disordered* by random anisotropy. The analysis is based on an expansion of Volovik's original random field model for ^{3}He-aerogel. I argue that the random anisotropy field results from mesoscopic structures in silica aerogels, coarse grained on the atomic scale, and formulated in terms of local anisotropy in the scattering of quasiparticles in an aerogel with orientational correlations. Long-range order of locally anisotropic scattering centers is responsible for the splitting of the transition for 1D and 2D orbital states.

Further tests of this theoretical description of anisotropic pair breaking, random anisotropy, and the stability of unique orbital phases of superfluid ^{3}He are possible with transport experiments on the same, or similarly prepared, anisotropic aerogels.

ACKNOWLEDGMENTS

This research is supported by the National Science Foundation (Grants No. DMR-0805277 and No. DMR-1106315). I thank S. Ali, supported on this project, for developing the DLCA code used to generate simulation images of the nanoscale structure of 98% aerogel. I acknowledge many discussions and explanations of experiments on ^{3}He in anisotropic aerogels with B. Halperin, J. Pollanen, J. Li, J. Parpia, and V. Dimitriev, as well as illuminating discussions on this work with V. Mineev. I acknowledge the hospitality and support of the Aspen Center for Physics where part of this work was carried out.

[1] J. V. Porto and J. M. Parpia, Phys. Rev. Lett. **74**, 4667 (1995).
[2] D. T. Sprague, T. M. Haard, J. B. Kycia, M. R. Rand, Y. Lee, P. J. Hamot, and W. P. Halperin, Phys. Rev. Lett. **75**, 661 (1995).
[3] J. Pollanen, K. R. Shirer, S. Blinstein, J. P. Davis, H. Choi, T. M. Lippman, W. P. Halperin, and L. B. Lurio, J. Non-Cryst. Solids **354**, 4668 (2008).
[4] A. J. Leggett, Rev. Mod. Phys. **47**, 331 (1975).
[5] J. Pollanen, J. I. A. Li, C. A. Collett, W. J. Gannon, and W. P. Halperin, Phys. Rev. Lett. **107**, 195301 (2011).
[6] R. Balian and N. R. Werthamer, Phys. Rev. **131**, 1553 (1963).
[7] H. Choi, K. Yawata, T. M. Haard, J. P. Davis, G. Gervais, N. Mulders, P. Sharma, J. A. Sauls, and W. P. Halperin, Phys. Rev. Lett. **93**, 145301 (2004).
[8] S. N. Fisher, A. M. Guenault, N. Mulders, and G. R. Pickett, Phys. Rev. Lett. **91**, 105303 (2003).
[9] J. A. Sauls, Y. M. Bunkov, E. Collin, H. Godfrin, and P. Sharma, Phys. Rev. B **72**, 024507 (2005).
[10] P. Sharma and J. A. Sauls, J. Low Temp. Phys. **125**, 115 (2001).
[11] E. V. Thuneberg, S. K. Yip, M. Fogelström, and J. A. Sauls, arXiv:cond-mat/9601148v1.
[12] E. V. Thuneberg, S.-K. Yip, M. Fogelström, and J. A. Sauls, Phys. Rev. Lett. **80**, 2861 (1998).
[13] K. Aoyama and R. Ikeda, Phys. Rev. B **73**, 060504 (2006).
[14] C. L. Vicente, H. C. Choi, J. S. Xia, W. P. Halperin, N. Mulders, and Y. Lee, Phys. Rev. B **72**, 094519 (2005).
[15] R. Bennett, N. Zhelev, E. Smith, J. Pollanen, W. Halperin, and J. Parpia, Phys. Rev. Lett. **107**, 235504 (2011).
[16] P. W. Anderson and P. Morel, Phys. Rev. Lett. **5**, 136 (1960).
[17] W. F. Brinkman and P. W. Anderson, Phys. Rev. A **8**, 2732 (1973).

[18]"Stretched" aerogels are not mechanically strained. Anisotropy equivalent to uniform axial strain with $\varepsilon_{zz} > 0$ is achieved by radial shrinkage during the drying process. See Ref. 3.
[19]J. Pollanen, J. I. A. Li, C. A. Collett, W. J. Gannon, W. P. Halperin, and J. A. Sauls, Nature (London) **8**, 317 (2012).
[20]G. E. Volovik, J. Low Temp. Phys. **150**, 453 (2008).
[21]D. Rainer and M. Vuorio, J. Phys. C: Solid State Phys. **10**, 3093 (1977).
[22]E. V. Surovtsev and I. A. Fomin, J. Low Temp. Phys. **150**, 487 (2008).
[23]E. V. Surovtsev, J. Exp. Theor. Phys. **108**, 616 (2009).
[24]T. Kunimatsu, T. Sato, K. Izumina, A. Matsubara, Y. Sasaki, M. Kubota, O. Ishikawa, T. Mizusaki, and Y. M. Bunkov, JETP Lett. **86**, 216 (2007).
[25]P. Meakin, *Fractals, Scaling and Growth Far from Equilibrium* (Cambridge University Press, Cambridge, UK, 1998).
[26]J. V. Porto and J. M. Parpia, Phys. Rev. B **59**, 14583 (1999).
[27]T. Haard, Ph.D. thesis, Northwestern University, 2001.
[28]H.-S. Ma, A. P. Roberts, J.-H. Prévost, R. Jullien, and G. W. Scherer, J. Non-Cryst. Solids **277**, 127 (2000).
[29]H. S. Ma, R. Jullien, and G. W. Scherer, Phys. Rev. E **65**, 041403 (2002).
[30]A. Larkin, Zh. Eksp. Teor. Fiz. **58**, 1466 (1970) [Sov. Phys.–JETP **31**, 784 (1970)].
[31]Y. Imry and S. Ma, Phys. Rev. Lett. **35**, 1399 (1975).
[32]The nuclear dipole-dipole interaction breaks the relative spin and orbital rotation symmetry, but is of order $E_D \simeq 10^{-7}$ mK per atom and can be treated perturbatively (Ref. 4).
[33]D. Vollhardt and P. Wölfle, *The Superfluid Phases of ^{3}He* (Taylor & Francis, New York, 1990).
[34]N. D. Mermin and G. Stare, Phys. Rev. Lett. **30**, 1135 (1973).
[35]I neglect the particle-hole asymmetry correction of order $\delta\chi/\chi_N \simeq \Delta/E_f \simeq 10^{-3}$.
[36]W. F. Brinkman and H. Smith, Phys. Lett. A **51**, 449 (1975).
[37]R. Sh. Askhadullin, V. V. Dmitriev, D. A. Krasnikhin, P. N. Martynov, L. A. Melnikovsky, A. A. Osipov, A. A. Senin, and A. N. Yudin, J. Phys.: Conf. Ser. **400**, 012002 (2012).
[38]R. Sh. Askhadullin, V. V. Dmitriev, D. A. Krasnikhin, P. N. Martynov, A. A. Osipov, A. A. Senin, and A. N. Yudin, Pis'ma Zh. Eksp. Teor. Fiz. **95**, 355 (2012) [JETP Lett. **95**, 326 (2012)].
[39]M. C. Cross, J. Low Temp. Phys. **21**, 525 (1975).
[40]G. E. Volovik and V. P. Mineev, Zh. Eksp. Teor. Fiz. **81**, 867 (1981) [JETP **60**, 276 (1984)].
[41]C. H. Choi and P. Muzikar, Phys. Rev. B **40**, 5144 (1989).
[42]G. E. Volovik, JETP Lett. **63**, 281 (1996).
[43]The "strand" model describes scattering by *strands* or *disks*.
[44]A more general model for random anisotropy would also include the rate parameters w_0, $w_\perp, w_\parallel$ as random variables since the structure of aerogel is far from a model of identical impurities. There are, however, constraints on the rate parameters. For example, the scattering rate is non-negative for all relative orientations of the incoming and scattered momenta. This constraint implies $w_0 > 0$ and $w_0 \pm w_{\perp,\parallel} \geqslant 0$. Furthermore, the local scattering centers are typically *not* uniaxial, but biaxial, $w_{ij} = w_s\,\hat{\mathbf{s}}_i\hat{\mathbf{s}}_j + w_s\,\hat{\mathbf{t}}_i\hat{\mathbf{t}}_j + w_u\,\hat{\mathbf{u}}_i\hat{\mathbf{u}}_j$, and described by three principal anisotropy axes $\hat{\mathbf{s}},\hat{\mathbf{t}},\hat{\mathbf{u}}$ and corresponding rate parameters.
[45]J. Pollanen, S. Blinstein, H. Choi, J. P. Davis, T. M. Lippman, L. Lurio, and W. Halperin, J. Low Temp. Phys. **148**, 579 (2007).
[46]J. A. Sauls and P. Sharma, New J. Phys. **12**, 083056 (2010).
[47]A. A. Abrikosov and L. P. Gorkov, Zh. Eksp. Teor. Fiz. **39**, 1781 (1960) [Sov. Phys.–JETP **12**, 1243 (1961)].
[48]J. A. Sauls and P. Sharma, Phys. Rev. B **68**, 224502 (2003).
[49]The pressure-dependent Fermi liquid parameters of ^{3}He are taken from the "Helium Calculator" http://spindry.phys.northwestern.edu/he3.htm.
[50]E. V. Thuneberg, Phys. Rev. B **36**, 3583 (1987).
[51]J. I. A. Li, A. M. Zimmerman, J. Pollanen, C. A. Collett, W. J. Gannon, and W. P. Halperin, J. Low Temp. Phys. (2013), doi: 10.1007/s10909-013-0917-3.